Universidade de Évora - Instituto de Investigação e Formação Avançada
Università degli Studi di Roma "La Sapienza" Aristotle University of Thessaloniki

Mestrado em Ciência dos Materiais Arqueológicos (ARCHMAT)

Dissertação

On the use of in-situ spectroscopic techniques for the study of the provenance of historic ivories

Dorothy Claire Guevarra Parungao

Orientador(es) | Catarina Miguel

António José Candeias

João Pedro Martins de Almeida Lopes

Évora 2022

Universidade de Évora - Instituto de Investigação e Formação Avançada
Università degli Studi di Roma "La Sapienza" Aristotle University of
Thessaloniki

Mestrado em Ciência dos Materiais Arqueológicos (ARCHMAT)

Dissertação

On the use of in-situ spectroscopic techniques for the study of the provenance of historic ivories

Dorothy Claire Guevarra Parungao

Orientador(es) | Catarina Miguel

António José Candeias
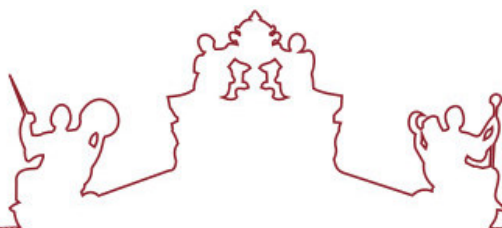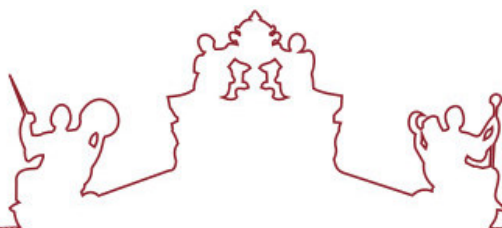
João Pedro Martins de Almeida Lopes

Évora 2022

A dissertação foi objeto de apreciação e discussão pública pelo seguinte júri nomeado pelo Diretor do Instituto de Investigação e Formação Avançada:

Presidente | Nicola Schiavon (Universidade de Évora)

Vogais | António José Candeias (Universidade de Évora)
Donatella Magri (Università degli Studi di Roma "La Sapienza")
Fabio Sitzia (Universidade de Évora)
Ioannis Karapanagiotis ()
Peter Vandenabeele (Universiteit Gent) (Arguente)

Évora 2022

UNIVERSITY OF ÉVORA

ARCHMAT

ERASMUS MUNDUS MASTER IN ARCHaeological MATerials Science

ON THE USE OF IN-SITU SPECTROSCOPIC TECHNIQUES TO DETERMINE THE PROVENANCE OF HISTORIC IVORIES

DOROTHY CLAIRE GUEVARRA PARUNGAO M47332

ANTÓNIO JOSÉ ESTÊVÃO GRANDE CANDEIAS

CATARINA AMÉLIA PEREIRA MIGUEL DE SOUSA CABRAL

JOÃO PEDRO MARTINS DE ALMEIDA LOPES

Évora, Portugal, November 2022

Acknowledgments

Abstract

Current protocols for ivory identification are destructive and resource-consuming. The current investigation aimed to develop a classification model based on *in-situ* spectroscopic techniques combined with chemometrics to discriminate between Asian and African ivory on the field. The spectroscopic techniques utilized were Fourier-transform Infrared Spectroscopy (FT-IR) and Fiber Optics Reflectance Spectroscopy (FORS) in the near-infrared region (NIR) combined with chemometric methods of Principal Component Analysis (PCA) and Partial Least Squares-Discriminant Analysis (PLS-DA). Historic ivories were successfully classified through FT-IR with PCA, and FORS-NIR with PLS-DA, resulting in a True Prediction Rate from 93.028% to 99.020% in African samples and 93.333% to 100.000% in Asian samples. The study demonstrated the potential of FORS-NIR as an investigative tool for ivory investigations. It also illumined the possibility of ivory trade networks of African ivory with the East, and a scientific perspective of the more desirable mechanical properties of African ivory over Asian ivory.

Resumo

Os protocolos atuais para identificação de marfim são destrutivos e consomem muitos recursos. A presente investigação teve como objetivo desenvolver um modelo de classificação baseado em técnicas espectroscópicas in situ combinadas com quimiometria para discriminar entre marfim asiático e africano no campo. As técnicas espectroscópicas utilizadas foram a espectroscopia de infravermelho com transformada de Fourier (FT-IR) e espectroscopia de reflectância de fibra óptica (FORS) na região do infravermelho próximo (NIR) combinada com métodos quimiométricos de análise de componentes principais (PCA) e análise discriminante de quadrados mínimos parciais (PLS-DA). Marfins históricos foram classificados com sucesso através de FT-IR com PCA e FORS-NIR com PLS-DA, resultando em uma Taxa de Previsão Verdadeira de 93,028% a 99,020% em amostras africanas e 93,333% a 100,000% em amostras asiáticas. O estudo demonstrou o potencial do FORS-NIR como uma ferramenta investigativa para investigações de marfim. Também iluminou a possibilidade de redes de comércio de marfim africano com o Oriente e uma perspectiva científica das propriedades mecânicas mais desejáveis do marfim africano sobre o marfim asiático.

Table of Contents

List of Figures

List of Tables

List of Abbreviations

CITES   Convention on International Trade in Endangered Species of Wild Fauna and Flora, also known as the Washington Convention

FORS   Fiber Optics Reflectance Spectrometry
FT-IR   Fourier Transform Infrared Spectrometry
ICNF   Instituto da Conservação da Natureza e das Florestas
NIR   Near-infrared region
PCA   Principal Component Analysis
PLS-DA   Partial Least Squares - Discriminant Analysis

Notes to Images

All images from the ICNF ivory collection were taken by Miriam Pressato.

All images attributed to São Roque Antiguidades e Galeria de Arte were taken from the book *From Lisbon to Japan: The Portuguese Empire in the 16th and 17th Centuries* published by São Roque Antiguidades e Galeria de Arte.

Icons used in the figures are courtesy of Flaticon.

Introduction

THE ELEPHANT(S) IN THE ROOM:

On the Use of In-situ Spectroscopic Techniques
to Determine the Provenance of Historic Ivories

Before the story of ivory unfolds, it helps to be guided by how the following introductory chapters are organized. It starts with an overview of the historical context of ivory, a state-of-the-art review of the identification of techniques in ivory, and the integrated methodology in this study.

INTRODUCTION

The Essence of **Ivory**

Ivory Across **Time and Space**
Ivory in the Ancient World
Ivory in the Age of Discovery
Ivory in the Machine Age

Ivory Trade in the
20th to 21st Century

REVIEW OF RELATED LITERATURE

The **present**
Current standard protocols
on the identification of ivory

The **past**
Early research
Radiocarbon dating and mulri-isotopic analysis
Combined and multianalytical approaches
Vibrational spectrometry

The **issue**
Problems with current techniques on the
identification of ivory
Experimental Design

METHODOLOGY

Ivories in Context
Historical Approach

Ivories on the Field
Scientific Approach

"Today, museums worldwide are home to thousands of ivory objects carved by artists from nearly every continent. These objects are multiple things at once. They are works of art, whether exquisitely carved or roughly hewn, and they are lessons in history both local and global."

Dr. Shannen Hill, in *The Art of African Ivory,* (2018)

The fate of African and Asian elephants has always been endangered by the historic demand for ivory that extends up to the present. Sophisticated techniques to identify both historic and confiscated ivory have been developed through the years as trafficking schemes grow more elaborate. However, a major issue about current protocols for ivory identification is that these are destructive to the sample, and tedious for multiple samples in ivory inspections. The current investigation aims to reverse the present workflow of bringing the ivory samples to the laboratory. Instead, the research proposes an efficient methodology and model that allows for a nondestructive but accurate large-scale identification of ivories on field. The methodology presented will focus mainly on the use of the techniques of vibrational spectroscopy, particularly Fourier-transform (FT-IR) spectroscopy in the External Reflection (ER) mode, and Fiber Optics Reflectance spectroscopy (FORS) in the near-infrared region (NIR), combined with chemometric methods. Aside from the scientific techniques, historic contextualization of the ivories will be established to aid in determining its provenance, context, and chronology.

The Essence of **Ivory**

Ivory Composition

Ivory is essentially the teeth and tusks of different animals, which are large enough to be processed and are of economic value (Espinoza and Mann 1999). Aside from mammoths and elephants, ivory can also come from narwhals, sperm whales, orcas, warthogs, and hippopotamus. Despite having many sources, ivory from elephants is highly sought because of its softness, texture and glean, and the lack of the tougher coating of enamel (Rosen 2012, 2), making them favorable for artists to carve (Wehrmeister et al. 2013). All teeth and tusks are composed of three basic structures: the pulp cavity, dentine, and cementum (Figure 1).

Collagen
+
Hydroxyapatite
$(Ca_{10}(PO_4)_6(CO_3)H_2O)$

dentine

molars

pulp cavity

cementum
(external layer only)

enamel
(tip only)
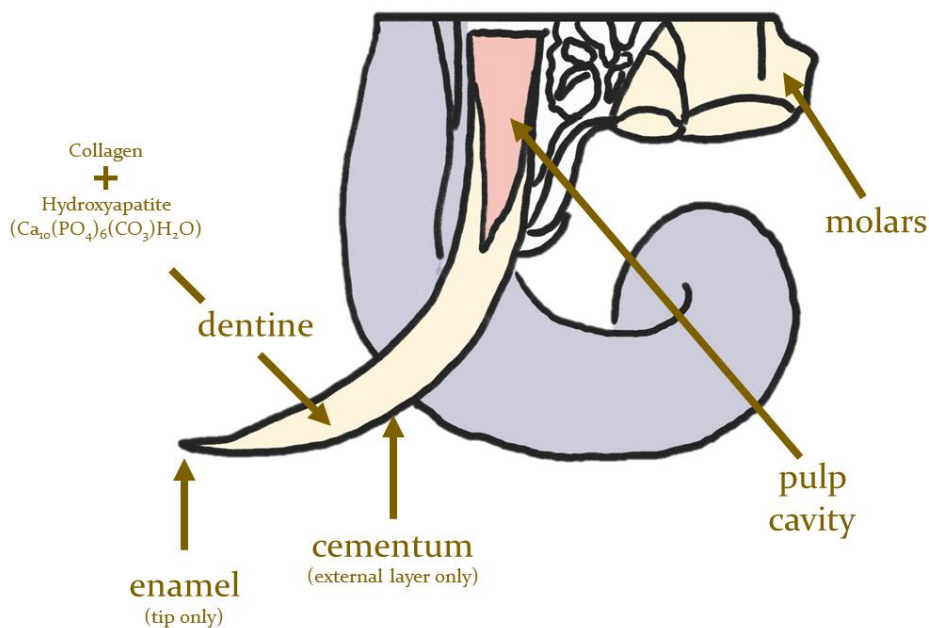
Figure 1. Tusk morphology diagram based on the illustration of Baker et. al (2020)

The innermost area is the pulp cavity. Here, the odontoblastic cells are found, which help in the production of dentine. The more significant part when considering carved objects is dentine, which is composed of an organic and an

inorganic component. The organic component is composed of collagen molecules, while the inorganic component is mainly hydroxyapatite ($Ca_{10}(PO_4)_6(CO_3)H_2O$). Lastly, cementum forms the layer over the dentine of tooth and tusk roots. When enamel is present, it caps the surface of the tooth or tusk and as the hardest animal tissue, also wears out the fastest (Baker et al. 2020, 5).

Elephant Species

Elephant ivory is sourced from three different kinds of elephants (Table 1). Ivory from these elephants differ in translucency, hardness, and chemical composition, which is influenced by the food eaten by the elephants, climatic condition of their habitat, and geology and soil composition of the area where the elephants live (Nocete et al. 2013).

Table 1. Summary characteristics of the elephant and mammoth species as ivory sources

Common name	Scientific name	Locations
Asian elephant	*Elephas maximus*	Majority in India, with some in Southeast Asia: Vietnam, Cambodia, and China (World Wildlife Fund 2022)
African savannah elephant	*Loxodonta africana*	Eastern and southern part of Africa, in the south of the Sahara desert (Bortolaso and Roth 2008, 39)

African forest elephant	*Loxodonta cyclotis*	Western equatorial Africa and Congo (Bortolaso and Roth 2008, 39)
Mammoth	*Mammuthus primigenius*	Extinct

Elephant Diet

The composition of ivory is largely determined by the elephant's physiology and diet, and the geochemical conditions of its habitat (Raubenheimer et al. 1998). Hence, it is necessary to consider possible differences in dietary habits and geochemical conditions of habitat between the Asian and African elephants to understand discrepancies in protein and water content. Elephants have been classified as "mega-herbivores" because of their enormous weight and their propensity to consume a wide variety of plant species. Depending on the seasonality and regional abundance, elephants eat fruits, bulbs, and roots, along with grasses, shrubs, and trees (Ullrey, 1997). Based on their predominant diet, they can be classified as "browsers" or "grazers". Browsers generally eat leaves, fruits of high-growing woody plants, soft shoots, and shrubs. Grazers, on the other hand, feed on grass and other low-lying vegetation. Depending on the season, African and Asian elephants can both be browsers and grazers. During the wet season, both species tend to graze on forbs and sedges, while in the dry months, they prefer to browse on barks, wood, and twigs (Wing and Buss 1970; De Boer et al. 2000; Mohapatra et al. 2013). For Asian elephants in Nepal, Koirala et al (2016) discovered that browsed species were preferred during the dry season while a combination of browsed plant species and grasses are also important during the rainy season. A study by Cerling et. al (1999) also revealed that Asian elephants might ingest a higher proportion of grasses than Africans despite the seasonality, making them grazers in general. Asian elephants prefer palms, grasses, and bamboo to tree saplings

(Terborgh et al. 2018). There was also a difference between the African savannah (*Loxodonta africana*) and African forest (*Loxodonta cyclotis*) elephants—the former being mixed feeders (grazers and browsers) and the latter, grazers. However, African forest elephants have also been shown to expand beyond the forest into the grasslands (Meyer, Honig, and Hadly 2022).

Ivory Across **Time and Space**

Through the procurement and carving of ivories, it does not only become an animal product, but a vessel of social, economic, and cultural meanings from its context of production. As raw and carved ivory follow along the trade routes, the inherent meanings associated with its production do not change, as for instance, in the case of African ivory, these are "African works that were produced in African contexts, following local patterns and involving local meanings, regardless of European presence" (Horta, Almeida, and Mark 2021, 21). The goal of this section is to reveal the possible trade networks that allowed for the exchange of ivory between the East and the West from the ancient world to the present. In resolving these spatial and temporal networks, it becomes manageable to bridge the gap between style and context of production—that is, connecting certain typologies present in the carved ivories to the communities that produced it. In this way, establishing the historical context is integrated within the whole methodology of identifying if the ivory is African or Asian. However, care must be taken as to misassign the ivory objects based on its artistic features alone.

Ivory in the Ancient World

In Southwestern Germany, the discovery of an ivory Venus figurine during archaeological excavations–along with ivory flutes and other sculptures–attest to humans' use of ivory for at least 35,000 years (Conard 2009).

Figure 2. The Venus of Hohle Fels. Photos by H. Jensen; copyright, University of Tübingen.

Later, in ancient Egypt, Mesopotamia, Greece, and Rome, ivory was used to craft furniture, boxes, jewellery, and figures. During this time, tusks were imported not just from Africa, but from as far away as Ceylon. The Arab navigators were crucial in facilitating this exchange between the East and the West. The workshops in Asia were primarily responsible for procuring their local source of ivory until the modern period, but East African ivory was also transported to India and China due to their high demand (Chaiklin 2010, 535). If these Asian countries have their own supply of ivory, why is there a need to acquire East African ivory? Primarily, African tusks were bigger compared to their Asian counterparts (Chaiklin 2010, 535). Moreover, both female African elephants carry tusks, while only male Asian elephants have them (Walker 2010). The trade between Africa and Asia as early as this period has been evidenced by a tenth-century account from the Arab geographer al-Masudi:

> It is from this [Zanj] country that come tusks weighing fifty
> pounds and more. They usually go to Oman, and from
> there are sent to China and India. This is the chief trade

route, and if it were not so, ivory would be common in

Muslim lands (Walker 2010).

If African ivory has been transported to Asia as early as the tenth century, ivory from India was also transported to Europe. The Phoenicians were mainly responsible for this exchange that occurred in the ancient Western world (Chaiklin 2010, 536).

China, meanwhile, imported their ivory mainly from South and Southeast Asia. Even in Japan where there are no indigenous elephants, ivory objects have been found in the Shōsōin—a storehouse dedicated to the articles of Emperor Shomu in 756—in which they were imported to and crafted in Japan. This influx of ivory into ancient Japan was made possible by diplomatic missions from China and Korea (Chaiklin 2010, 535) from at least as early as the sixth century. Domestic objects characterized this period of ivory carving in ancient Japan, most often reserved for the wealthy (Walker 2010).

Ivory for God

When Rome fell in 476, along also came the fall of ivory trade for several hundred years. Objects usually carved in ivory were now carved from the poor man's ivory: bone (Walker 2010). Another alternative was also preferred: walrus ivory, also known as "morse", for its intricate flame-like pattern (Chaiklin 2010, 536).

Spanning the eighth to the twelfth centuries was a time when ivory started to be used as a material for ecclesiastical and liturgical ensemble. Ivory was utilized to create beautiful book covers, ornamental plaques, holy water buckets, and oliphants (Guérin 2010, 1). The importance of ivory was established during

the ninth and tenth centuries as it was used for reliefs of sacred book covers and diptychs, which also cross-functioned as small shrines (Walker 2010). Ivory supply dwindled during the twelfth century, but the centuries after saw the golden age of Gothic ivory carving, from about 1230 to 1380. There was a new range of ivory object types: statuettes and statuette groups for the church or private home, miniature paneled objects known as diptychs (two panels), triptychs (three panels), and polyptychs (many panels). Ivory used during this period was primarily from the African Savannah elephant, and not from the Asian elephant of the Indian subcontinent (Guérin 2010, 1).

Figure 3. Example of a diptych, entitled "Diptych with the Coronation of the Virgin and the Last Judgment" ca. 1260-70. From the MET museum web catalogue.

Ivory in the Age of Discovery

Ivory for Glory and Gold

The Age of Exploration, 15th to the 17th century, saw a significant increase in the volume of ivory trade. While ivory was used for religious items during the Middle Ages, Europeans utilized ivory for navigational, scientific, and medical instruments. It was preferred for its carvability, resistance to shrinkage, ease of

cleaning, and a shiny white surface that allowed for high-contrast notation and numbering (Chaiklin 2010, 536).

The Portuguese Voyages

The first European power able to navigate around the Cape of Good Hope and across the Indian Ocean was the Portuguese. It started when Infante Dom Henrique (Henry the Navigator) of Portugal (1394-1460) sponsored journeys to Africa in pursuit of God (Christianity), gold (ivory and slaves), and glory (lands). At first, these journeys were a monopoly of the Crown, but as these tours became more profitable, the private merchants were licensed to participate. In the late 15th century, Portuguese ships replaced the traditional trade networks based upon caravans that came from the Levant to source ivory to Europe. Ivory was gained through trade rather than violence and hunts (Chaiklin 2010, 536). The extensive profits gained upon embarking on these voyages have encouraged other European powers to partake in the ivory trade. For instance, Dutch merchants have caught up to the Portuguese trade by the early 17th century. Upon the late 17th century and early 18th centuries, this ivory trade network extended along the length of the West African Coast, from Senegal to Cameroon and to Angola (Chaiklin 2010, 536.). While South Africa is rarely mentioned as ivory source at this period, ivory was procured here at least through the 19th century. It was also peculiar that this is the only place where foreign hunters actively hunted elephants for their ivory (Chaiklin 2010, 537).

While some sources say that East African ivory was exploited only by local networks by the Gujarati Indians until the late 19th century (Chaiklin 2010, 537), some sources posit that high demand for East African ivory in India and China is

already present from the 10th century into the 19th (Walker 2010). Evidence for centers of the ivory trade and ivory-working found itself within the interior of Africa, including the north bank of Zambezi (presently Zambia), and in the Limpopo Valley (South Africa today). There was also the addition of Abyssinia (today Ethiopia) into existing trade networks. All of these pushed the Indian Ocean ivory trade for international markets in the East and in Europe (Walker 2010).

Afro-Portuguese Ivories

Most of the ivory that the Portuguese brought back to Europe during the 15th to 16th century came from the West African coast, the Sapi area of Sierra Leone, and Benin, including the Kongo kingdom in Central Africa. In certain regions like the Edo kingdom of Benin (presently southern Nigeria), ivory was reserved for the exquisite ceremonies of the oba, the highest of titled chiefs and divinely appointed (Walker 2010).

The term "Afro-Portuguese ivories" is attributed to William Fagg, as he established in his book, *Afro-Portuguese Ivories* (Fagg and Fagg 1959). Here he described the identity of a unique art-form in a number of ivory objects—spoons, horns, saltcellars, oliphants—that was a hybrid of European form and function but carved according to the African artist. Fagg has hypothesized that this ivory design is attributed to the African tribe of Yoruba along the Slave Coast. However, some sources have refuted this claim as the typical ivory carving features limit them to the sixteenth century, even before the Portuguese frequented the Whydah-Lagos coast. It was also established that the ivory trade here was with Brazil, and not Portugal (Ryder 1964).

Yoruba Culture

When the Portuguese arrived at the West African coast in 1442, they were in contact with sophisticated societies that had been creating artistic figurines out of wood, bronze, copper, and ivory. Turns out, these local societies were the three ancient kingdoms of Owo, Benin, and Ijebu, which were at the heart of Yoruba culture. The Oba, supreme King or Ruler, was imbued with divine powers and preceded all community ceremonies. Developing ties with these highly organized societies, the Portuguese came to settle in this region from the middle 15th century. As an envoy from King D. João II, the Portuguese explorer João Afonso Aveiro (c.1443 to c.1490) landed in Benin, later to be accompanied by the Oba to Portugal, to promote the economic development and trade between two kingdoms, which included the exchange of ivory, copper, slaves, pepper, textiles, and bronze artifacts (Ferreira 2019c, 28–29). Hence, a hybrid art form was born.

Figure 4. Yoruba bracelet made for an Oba. Nigeria, probably 18th century. Image from "Lisbon to Japan, the Portuguese Empire in the 16th to 17th Centuries" (2019)

.

For further reading, a notable doctoral manuscript on the artistic-historical and material studies of 16th to 17th century Luso-African ivories from the kingdom of Benin, also known as "Afro-Portuguese" has been conducted by Amaral (2022). This places the ivories in the context of "proto-globalization" that synthesizes the context of their production and the origins of the kingdom of Western Africa.

India: Indo-Portuguese Ivories

During the Age of Discovery, India was crucial for cultural and religious dissemination in Asia. It served as a melting pot that received the European Christian faith, Hinduism, Buddhism, Islam, and even raw materials and goods like African ivory from Mozambique or porcelain from China. When the Portuguese conquered Goa in 1510, they designated it into a chief trading center and principal nexus between South and North India, connecting it to Persia through Ormuz, and to China and the rest of Southeast Asia through Malacca. Aside from seizing the means of trade, the Portuguese also aimed to propagate Christianity to the locals. While Goa was an important trade center, it was also a prominent artistic center as well, receiving the influx of luxury Asian goods. This is how Goa became a production center for small-scale sculptures and ivory objects, and this was exploited by the Portuguese to assimilate the Christian faith into the natives. Carvers were commissioned to infuse Christian images and biblical figures with the local religion into the ivory carvings to make it easier for the locals to accept the faith. In fact, Asian features were also incorporated as they followed European prototypes. Hence, a hybrid art form, Indo-Portuguese art, was born. Primarily only the local craftsmen were commissioned to do the

ivory carvings, but soon enough, merchants and craftsmen from various cultures from Europe to the Far East would also live in Goa (Ferreira 2019a, 28–29)

Images that would be representative of Indo-Portuguese art would be the image of Christ as a Good Shepherd, and elements of Mannerism, as adopted from the Portuguese *Manuelino* (Ferreira 2019a, 28–29). The Manueline style is an ornate form of architectural ornamentation native to Portugal in the early 16th century. Its representative elements are deliberately nautical, as the Portuguese were a nautical power then. Carved barnacles or seaweed and algae encrust the moldings, while heraldic shields, crosses, anchors, navigational instruments, and buoys decorate the windows and doors (Tikkanen 2022).

Figure 5. Polychrome ivory of the Archangel Michael slaying the Demon. Indo-Portuguese origin, 17th century. Image from "Lisbon to Japan, the Portuguese Empire in the 16th to 17th Centuries" (2019).

China: Sino-Portuguese Ivories

The relations between Sinhalese-Portuguese relations traces back to the trade of Portuguese merchants along the coastal regions of Asia and in crucial ports such as Malacca, Canton, and Fujian, in the early 16th century during the

Ming Dynasty (1368-1644). These relations were then improved by the establishment of a Portuguese colony in Macau (1544). It was in the same period that China became an important center for the conversations between religious syncretism and artistic cultures. Primarily, this religious fusion of Christianity and the two main religions, Buddhism and Taoism, manifested itself in commissioned ivory pieces crafted by indigenous craftsmen (Ferreira 2019c, 132–33).

A notable example of the imbuement of sacred Chinese subjects into European-commissioned sculptures was the ivory sculptures between Virgin and Child, with strong parallels with the Chinese goddess Guanyin, who is also depicted as a maternal figure holding a child on her lap. Representations of the Virgin Mary and Christ as *Salvator Mundi* served a function "as the standards of the mission to disseminate Christianity throughout the New World", according to Matteu Ricci. He then presented an image of the Virgin and Baby Jesus to the emperor Wanli in 1601 (Ferreira 2019d, 132–33).

Figure 6. Image of the Virgin and Child, notable image in the south of China where it is associated with the cult of Guanyin. Sino-Portuguese 16th to 17th century. Image from "Lisbon to Japan, the Portuguese Empire in the 16th to 17th Centuries" (2019).

Thailand: Siamese-Portuguese Ivories

Thailand has had a long history that was untainted by the colonization of the Portuguese and any European power. Thus, the relationship between the Thai and the Portuguese is based upon a solid commercial and diplomatic relations of equals. These relations find its origins in the conquest of Malacca in 1511 by the Portuguese explorer Afonso de Albuquerque, which was previously held as a vassal of the Siam king. The Emissary Duarte Fernandes was sent by the Viceroy of India as a courtesy visit to the Siamese capital Ayutthaya. Subsequently the King of Siam offered a parcel of land from Ayutthaya, enabling the growth of a Luso-Siamese community known as *Bang Portuguet* or the Portuguese Quarter of Ayutthaya, free from commercial taxes and religious restrictions (Ferreira 2019b, 152–53).

The hybrid artistic language of the fusion of Christianity with Buddhism manifests itself in images of the Good Shepherd in fusion with images of Buddha. Oftentimes this is revealed in sculptures of the reclining infant Christ, with a position similar to the Buddha or Shiva (Ferreira 2019b, 152–53).

Figure 7. Baby Jesus ivory produced in a late 16th century in a Luso-Siamese workshop. The spiralled hair and reclining position alludes to the Buddha. Image from "Lisbon to Japan, the Portuguese Empire in the 16th to 17th Centuries" (2019).

Ivory in the Machine Age

Decreases in Elephant Population

It was in the 19th century that ivory was related to slavery, mainly because they were both sold in the same ports that led to the same distribution networks. With ivory having the highest export value from East Africa during the entirety of the century, ivory was deemed more important than anything else, having earned the moniker "white gold" (Chaiklin 2010, 538–39).

Aside from new trade networks, there were other important factors that affected the population of elephants: (1) the propagation of large elephant guns, and (2) the extensive land use carried upon by colonization. The first reason resulted in an increase in hunting for ivory and sport, of which the goal was to obtain trophies. Frequently these trophy hunters were foreigners to the area and seemed to proliferate more in Southeast Asia than in Africa. On the other hand, extensive land use brought about a decrease in the habitable areas for elephants. For instance, elephants were deliberately culled to protect fields from being trampled upon. All these factors contributed to the intensely diminishing of elephant populations—extensive trade networks, unselective butchery, and habitat destruction for the elephant (Chaiklin 2010, 538–39).

A Revolution in Ivory Production

Before the 19th century, ivory carvers utilized a variety of rasps and chisels. Even before that, lathes were also widely used (Chaiklin 2010, 548). It was until the 19th century that two machines revolutionized the ivory carving industry. A man named Deacon Phineas Pratt issued a patent for a comb-making machine. Consisting of flywheels and fan belts, thin circular saws and adjustable precision

clamps on a wooden stand, it cut the time needed to nick the teeth of combs (Walker 2010). This laid out the foundation for the manufacture of the most popular ivory object in history: combs. Another machine that revolutionized ivory production was the veneer cutting machine, first patented by H. Pape in 1826 (Chaiklin 2010, 540). At the peak of ivory production, it has become the "plastic" of the 19th century. Plastic substitutes have been established to replace ivory, which worked better for some materials like billiard substitutes due to their exact center of gravity. However, ivory worked better for piano keys which would prevent a slippery surface due to oil and sweat (Chaiklin 2010, 540).

Machining Ivory

Before tusks are machined, an ivory selector inspects the sample ivories and divides them roughly into "soft" or "hard" ivories—which depends on appearance and workability (Walker 2010). The preferred material for carving was soft ivory from East Africa, much so because it is easily cut and worked. Its premium quality that comes at a lower cost made it much sought after in the East and in Europe since the Middle Ages. The biggest development in the demand for soft ivory coincided with the opening up of East Africa to Arab traders and European explorers, which led to the further exploration of ivory in the interior (Beachey 1967, 269). Up until the end of the 19th century, East Africa was the main global source of ivory, of which export value topped the competition (Beachey 1967, 270).

Prior to being cut, tusks are washed, reweighed, marked with an order number, and soaked in a bath of peroxide. Tough stains are removed from the ivory by the bleaching process of hydrogen peroxide in water. Then, tusks are

placed in the "junking" machine, which divides it into four-inch-high cylindrical chunks. Cutting at right angles also created a lot of circular waste wedges. "Junkers" should take care not to hit the musket ball deep within the tusk. After that, each piece is placed inside a box and covered with damp cloth. Each is stored in foreman's cupboard and he in turn had the responsibility of scoring the flat part of the tusk to produce the maximum number of products, say piano key covers. Then, he hands it over the next worker and the process culminates in an ivory product (Walker 2010).

Ivory Trade in the **20th to 21st Century**

"One sees all sorts of knives on the day an elephant

dies."

- Yoruba proverb

Ivory and the Elephant

With the significant downward trend of elephant populations caused by the drastic changes that occurred during the 19ᵗʰ century, it becomes necessary to consider the relationship between the ivory and the elephant. Moreover, this step is necessary to get to the heart of the conservation dilemma. Consequently, the ivory trade depends on the demand for ivory, which is inherently linked to the supply of elephants. In this section, the current population and conservation status of the elephants are discussed, along with a brief historical overview, followed by the human toll of ivory, and a current overview of the trends in the ivory trade. The goal of this section is to highlight why the identification of ivory can be beneficial to curb a channel in the global ivory black market.

Population and Conservation Status of the Asian and African Elephant

A decreasing population trend estimates that there are 46,000 individuals in the wild for the Asian Elephant, in which over 50% of the remaining are in India (Jirik 2021). It is still listed on the Appendix I by CITES, is classified as Endangered by the International Union for the Conservation of Nature (IUCN), and Critically Endangered for the Sumatran elephant subspecies.

The African elephant has recently been categorized as Endangered (African forest elephant), and Critically Endangered (African savannah elephant) ("Poaching behind Worst African Elephant Losses in 25 Years – IUCN Report" 2016).

This puts the estimated population at around 415,000 elephants in the wild for both species (2021).
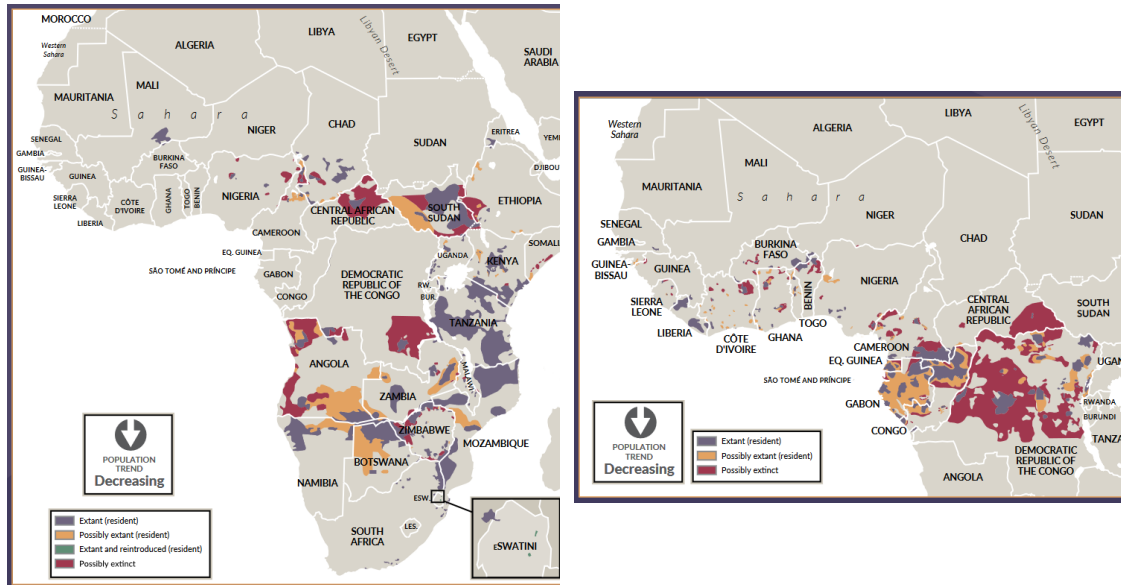
Figure 8. Present distribution of the African savannah Elephant (a) and the African forest elephant (b). Both have a decreasing population trend according to IUCN's latest report (2021)

Figure 9. Latest distribution of the Asian elephant according to IUCN report. The species is also classified as endangered (IUCN 2018).

Two Important Decisions

It was in the 18th to the 20th century that the demand for ivory became thoroughly unsustainable. It was considered as the "new plastic" of its age, as it was used in everyday items, billiard balls, and piano keys (Walker, 2010). This prompted the formation of the **Convention on International Trade in**

Endangered Species of Wild Fauna and Flora (CITES) in 1973, which lists three levels of concern for endangered species–Appendix I being the most stringent, and Appendix III being the least. With this, the **Endangered Species Act (ESA)** was also signed into law in the United States and became immediately effective. The **Asian elephant** was listed on CITES Appendix I in 1975, which fully bans the international commercial trade of ivory. However, ivory owned before this year is considered as "pre-Convention". This means that it can be traded internationally without a valid CITES documentation. The Asian elephant was listed under the ESA in 1976, and ivory possessed before this year is considered as "pre-Act" and can be sold domestically within the US. Both are legal loopholes that smugglers invoke at present. Meanwhile, the **African elephant** was listed on CITES Appendix II in 1977, in which international trade is allowed if exporting countries monitor that the species is not endangered. However, the regulated trade proved to be a failure and the import of African elephant ivory to the US for commercial purposes was banned in 1989. The regulated trade enabled the drastic reduction of the African elephant population by half from 1979 to 1989–from an estimated 1.3 million to 600,000 at the end of the decade (Humane Society International 2014). This crisis prompted CITES to list the African elephant on Appendix I in 1990, banning the international commercial trade of African ivory globally. In the same year, only Botswana, Namibia, and Zimbabwe were allowed to list the African elephant under Appendix II, with an "annotation" that international trade is not allowed for commercial purposes. In 1997, the **Elephant Trade Information System (ETIS)** was established to monitor and analyze illegal ivory trends. Around the same time, its sister program, **Monitoring the Illegal**

Killing of Elephants (MIKE) was also established to track elephant poaching on the ground across Africa and Asia (Humane Society International, 2014).

After this period, experts believe there were two controversial decisions that changed the fate of elephants forever. These were the **one-time sales** of 49 metric tons of government-stockpiled ivory from Botswana, Namibia, and Zimbabwe to Japan in 1999, and of 102 metric tons of ivory from the same countries including South Africa, to China and Japan in 2008, called "The Japan Experiment". Globally, experts have dubbed the experiment as a failure ("How Japan Is Fueling the Slaughter of Elephants" 2015), with a 66% increase in illegal ivory production across Africa and Asia, and an estimated 71% increase in ivory smuggling out of Africa after the legal ivory sale (Hsiang and Sekar 2016). The black-market activity that may or not have been aggravated by the one-time sale has been unregulated mostly because legal ivory cannot be distinguished from illegal ivory.

Ivory as a Currency of Terror in Africa

While ivory has been dubbed as "white gold", its long history has always been tied to the history of slavery, exploitation, and terrorism. It is necessary to not only consider the toll of ivory in elephants, but also its human toll. This has earned it its other nickname, "blood ivory". After the one-time sales, poaching incidents peaked during 2011 to 2013. It was also at this time that Bryan Christy of the National Geographic had an idea: to hide GPS trackers in fake tusks that would be infused into the supply chain. His year-long investigation to track the illegal tusk trade of Africa's most notorious militias and terrorist organizations was chronicled in National Geographic's groundbreaking documentary, *Warlords of Ivory* (2015). The fake tusks were

planted in the southeastern Central African Republic, at the heart of the supply chain. Through South Sudan, the tusks entered Kafia Kingi, a disputed territory controlled by Sudan and believed to be a home base for the Lord's Resistance Army, led by ICC fugitive and war criminal Joseph Kony. As it moves through the supply chain in Africa, its price could rise up to tenfold, from $66 to $882. Christy's fake tusks travelled for a total of 592 miles (953 km) before getting buried or kept inside a building. Due to the high level of corruption and lack of border control, transnational criminal organizations and armed groups are able to avoid being detected and prosecuted (Action for Elephants UK 2018).

When it reaches Asian markets, the price can skyrocket from $946 to $4630. Demand for ivory is concentrated in China, Thailand, Vietnam, the Philippines, and the United States. Demand for ivory has also moved from being an investment onto a symbol of status among China's middle-class (Strauss 2015).

However, a recent study by Duffy (2022) shifts the focus from the militarization of Africa's conservation policies to the struggle of the marginalized peoples. It explains the nuances of why there was a shift towards more punitive conservation policies—a combined sense of urgency about poaching, about organized crime networks, interests of the world's political elite, and highly competitive government funding for NGOs. It asserts that there are multiple dimensions to be considered when tackling ecological and wildlife problems—and being cautious about reducing ivory, or any wildlife, solely to a currency for terror.

The Ivory Trade Today

There is hope for the elephant today. Elephant poaching rates in Africa have begun to decrease after a peak in 2011, from an annual poaching mortality rate of over 10% in 2011 to less than 4% in 2017 (Hauenstein et al. 2019). The CITES MIKE Programme also reported a continued downward trend in elephant poaching in Africa in its latest memorandum report in 2020 (CITES 2020). A rapid assessment of the Illegal Wildlife Justice Commission in 2020 has also seen that values of raw ivory have followed a decreasing pattern since 2017 (Wildlife Justice Commission 2020). However, this should not be interpreted immediately as a decrease in poaching rate since there was an identified relationship between trade in ivory and trade in pangolin scales. An analysis conducted by the Wildlife Justice Commission in 2019 also analyzed that while the ivory prices are dropping, pangolin scales are not (Wildlife Justice Commission 2020). This suggests that the focus has been on the trafficking of pangolin scales during the past few years. While the recent trends show an optimistic future for the elephant, it should not be a reason to be complacent. More so, investigations and regulatory measures must be more focused and efficient since ivory seizures have more than doubled in 2019 (Wildlife Justice Commission, 2019). This is also combined with the decreasing population trend observed for both the Asian and African elephant.
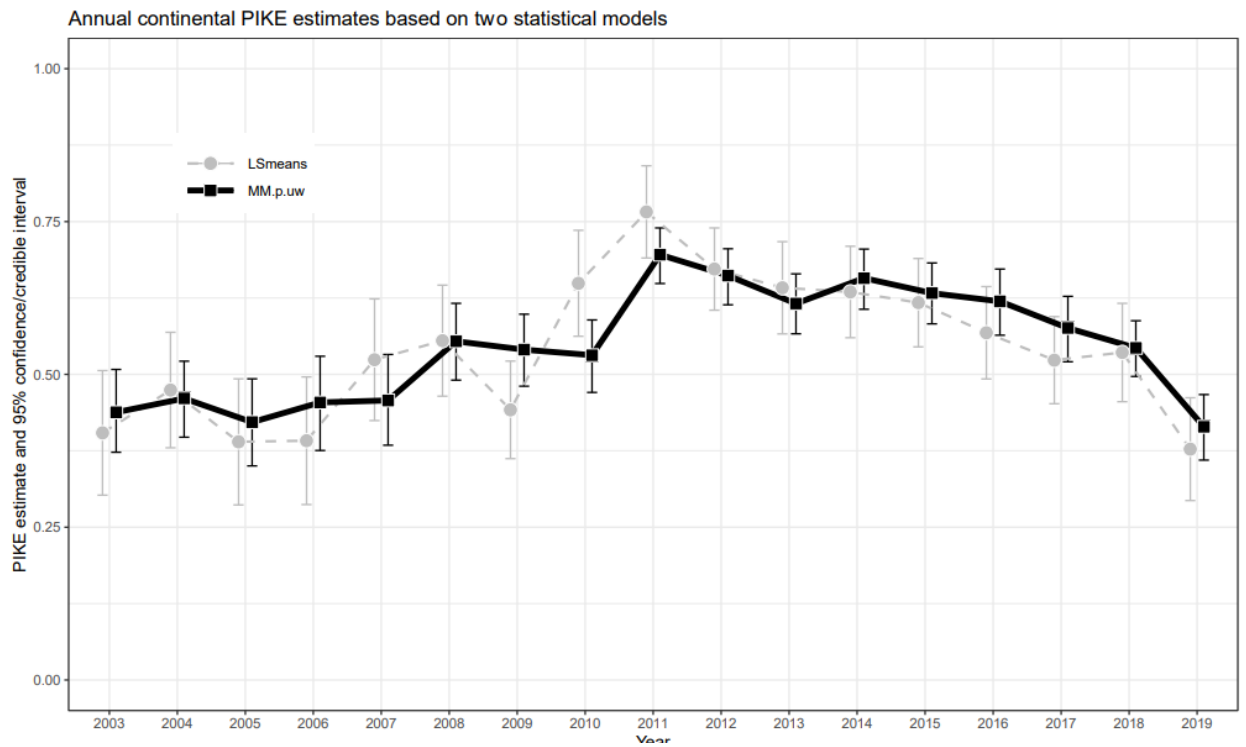
Figure 10. Proportion of Illegally Killed Elephants (PIKE) trend analysis from 2003 to 2019 by the MIKE Program. A downward trend has been observed for ivory seizures (proxy data) since 2017.

Review of Related Literature

Identifying Ivory

The legalization of the one-time sales in 1999 and 2008 made it harder for inspectors to distinguish legal from illegal ivory. Most smugglers exploit the legal loopholes of the "pre-Convention" and "pre-Act" ivories because there is currently no readily available way to readily determine the age and provenance of ivories in inspections.

Proboscidean ivory

Among other ivories, Proboscidean ivory is the easiest to distinguish visually. This type of ivory was named so from the order Proboscidea, which includes, but is not limited to, mammoths and elephants. A feature that is unique to Proboscidean ivory is the Schreger lines, named after Bernhard Schreger, who noticed this phenomenon initially in 1800. These are formed by microchannels within the dentine, which radiate outwards from the pulp cavity to the cementum border (Figure 11). These lines are dictated by gene control, hence can be diagnostic of the order (Nocete et al. 2013). The intersections of these Schreger lines form concave and convex angles called Schreger angles (Figure 11), which are acute in extinct Proboscidea (mammoth) and obtuse in extant ones (modern elephants) (H. Edwards 1998). While earlier studies (H. Edwards 1998; Nocete et al. 2013) were able to distinguish mammoth ivory from modern elephant ivory, recent ones were able to distinguish between African savannah ivory (average value of 118 degrees) and Asian ivory (average value of 112 degrees) (Nocete et al. 2013). The morphology of proboscidean ivory was also well-discussed by (Virág 2012). In this study, the Schreger line in Proboscidean ivory was modelled

as a sinusoidal undulation of the dentinal tubules in radial profiles in elephantoids – aptly called the "phase shift" model.

Figure 11. Microscopic and macroscopic diagrams for Schreger angles. Pictures taken from Baker et. al (2020) and Trapani and Fisher (2003).

The present: Current standard protocols in the identification of ivory

Since the ivory ban, protocols have evolved to identify ivories efficiently and conveniently. Features to consider go beyond the Schreger angles, and even encompass other types of ivories. As of 2020, laboratory protocols for ivory inspection and classification have been set by the International Consortium on Combating Wildlife Crime in the latest edition of the manual, *Ivory and Ivory Substitute Guide* by Baker et. al (2020). The first consideration is the form of ivory – if it is raw (unprocessed whole or sectioned tusk) or worked (including but not limited to carved ornaments, hankos, earrings, pendants, and netsukos). From there, the research questions are formulated based on the laboratory and skill

capacity of the responsible institution. These types of questions revolve around the identification of species, of age, of geographical origin, and of the number of elephants killed. Consequently, a methodology is formulated based on the research questions that need to be addressed (Table 2). Some techniques can answer more than one research question, and so, with a combination of techniques, research questions can be answered simultaneously.

Table 2. Summary of standard laboratory protocols for ivory and ivory substitute identification

Species identification	Age identification	Geographical origin identification
Morphology	Morphology	DNA analysis
Vibrational spectroscopy (Raman and FT-IR)	Isotope analysis (radioisotope)	Isotope analysis
	^{14}C, ^{90}Sr, $^{228}Th/^{232}Th$	
Mitochondrial DNA		

The past: Previous research on ivory identification

Early research

A plethora of research has been dedicated to the identification of ivory beyond solely the measurement of Schreger angles. Raubenheimer et. al (1998) were able to build a database of geographic variations in the ivory composition of the African elephant. A total of 20 elements were detected in the organic component with concentrations of calcium, phosphate, magnesium, fluoride, cobalt, and zinc showing statistically significant differences between ivory obtained from different African regions. The organic fractions also varied based

mainly on the environmental conditions of sunlight and rainfall distribution. Published in the same year, Burragato and co-authors (1998) proposed thermogravimetric analysis as a way of distinguishing elephant and mammoth ivory, with no pretreatments required. The team also used XRD and FT-IR but these techniques were not able to distinguish between the materials. Although it was, in retrospect, relatively low-cost and easy to read, a small sample of material (2-3 mg) needed to be destroyed. Around the same decade, FT-Raman spectroscopy was also utilized by H. Edwards (1998) to differentiate between mammoths and elephants (African or Asian) based on confiscated ivory samples in London airport.

Later on, Trapani and Fisher (2003) were able to analyze Schreger line features to go beyond distinguishing Proboscidean ivory, to interspecies of extant elephants (African or Asian). However, even the authors agree that the distinction between Asian or African ivories based on these methods is unreliable, due to the limited sample size and the available gender of species, since female elephants have a smaller tusk.

Radiocarbon dating and Multi-isotopic analysis

Like the current standard protocol, radiocarbon dating can be used to date ivory artifacts. This was used in the study of hippopotamus and elephant ivory artifacts in 16th century Portuguese shipwreck in Goa by Tripati and Godfrey (2007). Isotopic analyses were also commonly paired with radiocarbon dating to determine provenance and age of ivory. Multi-isotopic analyses also aided in explaining the variation in data and in testing the robustness of the datasets (Coutu, Whitelaw, et al. 2016). These dual analyses were used to determine the provenance of post-medieval African ivory in Amsterdam (Rijkelijkhuizen,

Kootker, and Davies 2015), to determine the trade networks of ivory in 20th and late 20th century East Africa (Coutu, Lee-Thorp, et al. 2016), and to distinguish legal from illegal ivory using an improved radiocarbon dating method (Schmidberger et al. 2018).

Combined and multianalytical approaches

Multianalytical approaches became more common later on for the identification of ivory. Singh and co-authors (2006) performed a comprehensive approach to distinguish Asian from African ivory using XRF, ICP-AES, and ICP-MS as preliminary methods. Here, isotopic analyses of carbon (for diet) and nitrogen (for rainfall) were used for confirmation, although nitrogen analyses produced more robust results. Additionally, Yin and co-authors (2013) were able to differentiate mammoth from modern elephant ivory using SEM, IR, and LIBS. Betts and co-authors (2016) characterized a heavily burnt and intricately curved solid material in Uzbekistan as African ivory using neutron tomography, and XRD. Through stable isotope analyses and radiocarbon analyses, they also determined the cylinder to be of nonlocal provenance. In another study, the ivory artifacts in Perdigões, Portugal's largest deposit of ivory artifacts, were traced to the African savannah elephant by Valera and co-authors (2015). They used optical microscopy (OM), IRMS, micro-computer tomography, and particle-induced gamma ray emission (PIGE) combined with functional and morphological analysis to characterize their provenance and determine their social role. In one study, Coutu and co-authors (2016) combined the multi-isotopic analysis of carbon, nitrogen, and strontium was combined with Zooms (Zooarchaeology by Mass Spectrometry) to explore the provenance and trading of ivory in South African sites. The bulk of the ivory was determined to be of elephant source

despite the abundance of hippopotamus in the area, suggesting a divide between landscape and resource management.

Vibrational spectroscopy

Perhaps the most notable body of techniques used in the identification of ivory is vibrational spectroscopy. In this discussion, the term vibrational spectroscopy encompasses Fourier-transform infrared spectroscopy (FT-IR) in the infrared and near-IR (NIR) regions, and Raman spectroscopy in the near-IR region.

a. Raman

The use of FT-Raman in the characterization of ivory has been well-studied, particularly by Howell G.M. Edwards. His research addressed how FT-Raman can be used for the distinction of ivory from its synthetic counterparts (H. G. M Edwards and Farwell 1995), a comprehensive spectroscopic assignment of molecular and vibrational bands to African, Asian, and mammoth ivory (H. G. M. Edwards et al. 1997b), and a protocol for the identification of mammalian specimens (sperm whale, walrus, warthog, narwhal, hippopotamus, and domestic pig) other than elephant and mammoth ivories (H. G. M. Edwards et al. 1997a). His recent research was concerned with the combination of FT-Raman with chemometric methods to study the biodeterioration of both ancient and modern Proboscidean ivory (Howell G. M. Edwards et al. 2005) and to identify the elephant species of the modern ivory artefacts (H. G. M. Edwards, Hassan, and Arya 2006). In one of the studies, the team of H. Edwards found out that the success of applying FT-Raman and chemometric methods to characterize ancient mammoth ivory (buried for 10 ky and 65 ky) was highly dependent on its specimen history and condition (Howell G. M. Edwards et al. 2005). Particularly,

the ancient mammoth ivory inspected here suffered greatly from the biodeterioration of its collagen and hydroxyapatite components. The problem of biodeterioration of collagen also persisted in the study by Long and co-authors (2008). In this study, the bands assigned to modern ivories were determined to be incompatible with ancient mammoth ivories because of their collagen degradation and the decrease of spectral quality. Other than Edwards, other research also combined FT-Raman with chemometric methods to distinguish African from Asian ivory with limited success (Brody, Edwards, and Pollard 2001; Nocete et al. 2013); and with unsuccessful attempts (Wehrmeister et al. 2013). Succeeding studies (Hargreaves et al. 2009) were able to compare the capability of mobile Raman spectroscopy and benchtop spatially offset Raman spectroscopy (SORS) techniques to efficiently distinguish real and fake ivory. With this research, the team was able to determine SORS was better in this regard because of its ability to identify ivory concealed by plastics, paints, varnishes, and cloth, in contrast to conventional Raman spectroscopy. In another interim investigation by O'Connor and co-authors, the application of FT-Raman, as a minimally-destructive dating technique, to date, cultural ivory objects were tested (O'Connor, Edwards, and Ali 2011). However, the researchers were able to determine that the vibrational spectra of ivory cannot be used to deduce the relative age of the samples. A study by Guennec (2020) revealed that FT-Raman 1064 nm can distinguish between subspecies of African elephants (forest and savannah) but not FT-Raman at 785 nm.

B. FT-IR

The use of FT-IR for the characterization and identification of ivory specimens has also been well-studied. ATR-IR microspectroscopy was

combined with curve-fitting methods to analyze bioarchaeological ivory (Céline et al. 2009) while FT-IR spectroscopy was used to discriminate between Asian and African ivory in studies by Nocete et al. (2013) and Guennec (2020), and between mammoth and modern elephant ivories (Yin et al. 2013). In some cases, FT-IR spectroscopy was determined to be an unreliable method for distinguishing African from Asian ivory (Cartier et al. 2020).

A previous investigation done by researchers of the HERCULES laboratory supervised by C. Miguel, allowed for the PCA clustering of ivories based on their FT-IR-ATR spectra (Figure 12). The results revealed promising prospects for investigation of ivories via spectrometric and chemometric methods, which would later become the basis for this research.

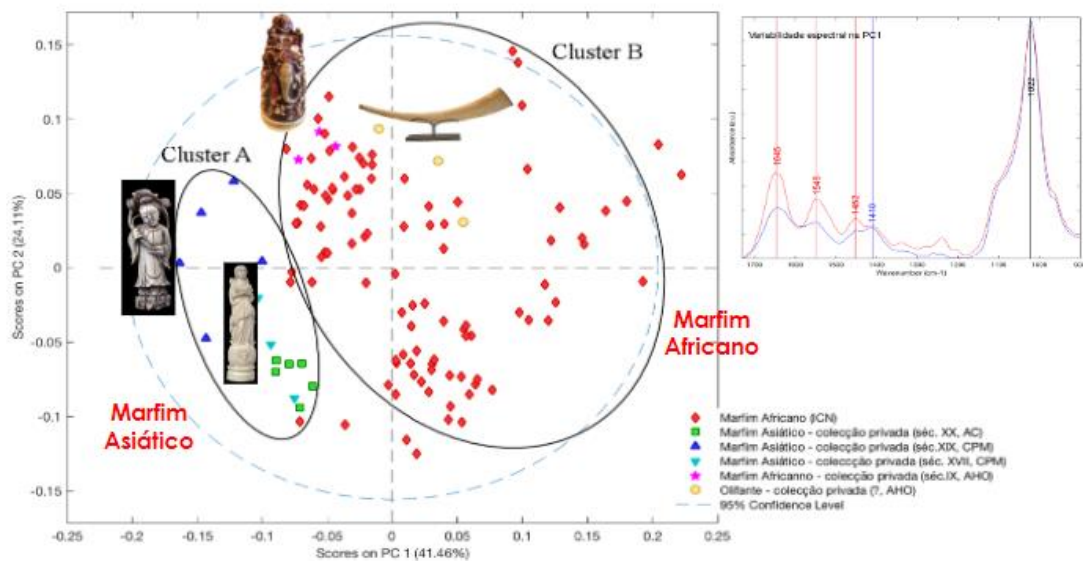*Figure 12. PCA score plot shows two clusters formed: Asian and African ivory. Loading plots show the relevant wavelengths responsible for the discrimination.*

C. NIR and Chemometrics

Another technique that has been well-documented in literature for the characterization of ivories is spectroscopy in the near-infrared region (NIR). This technique is usually combined with chemometric analyses like Principal

Component Analysis (PCA) and Partial Least Squares-Discriminant Analysis (PLS-DA) to aid in categorizing ivory artifacts. For instance, Fourier-transform near-infrared (FT-NIR) was used to characterize the tin and amber decoration on Iberian ivory artifacts from the Middle Age (Blasco-Martín et al. 2019)**.** The most notable use of NIR coupled with chemometrics was to discriminate between rhino horn and ivory samples from different mammalian species (A. Power et al. 2019) and to differentiate between Asian savannah, wild Asian, and domesticated Asian elephant ivories (Chaitae et al. 2021). As demonstrated by these studies, spectroscopy in the NIR coupled with chemometrics has great potential to be applied to the nondestructive procedure of ivory identification in the field.

The issue: Problems with current techniques in identifying ivory

In ivory trade inspections, it is difficult to determine provenance solely by visual inspections. Schreger lines are not enough to distinguish between ivories, especially if the samples are carved, unpolished, and cut in oblique angles (H. Edwards 1998; Wehrmeister et al. 2013). Because the common form of confiscated ivory is carved, there needs to be a method that is more reliable than the visual inspection of Schreger lines.

A more significant issue with the current techniques employed is that these are semi-destructive and time-consuming—hence, an efficient procedure is not yet available for inspectors on the field. It is difficult for the majority of stakeholders in the ivory industry, including the regulatory bodies and customs officers, to adopt the contemporary procedures due to various factors: costly implementation, their associated complexity of the *in-situ* applications, and the variability in the produced datasets (A. Power et al. 2019). It has become

increasingly important to conduct these ivory investigations, which encompass screening and routine inspections, in a nondestructive manner (Chaitae et al. 2021). Otherwise, the systems in place for regulating and controlling ivory trade are susceptible to the incorporation of illegal or noncompliant materials (A. Power et al. 2019). There needs to be an efficient methodology that goes beyond visual identification of Schreger lines that allow for the identification of their animal source, geographic origin, age (relative to the convention rules of what is illegal ivory and not), and possibly, the number of animals killed.

Experimental Design

This research aims to address this gap by developing an efficient and cost-effective methodology that would allow investigators to use analytical techniques in-field. In particular, it is aimed to investigate the potential of vibrational spectroscopic techniques that can be applied *in-situ* and nondestructively. The goal of the proposed workflow is that instead of bringing the samples to the laboratory, the laboratory techniques will be brought to the field. This will alleviate the issues of sample contamination and eliminate the complications of sample transport logistics.

Moreover, the choice of analytical techniques depends on its ease of transport to the field and its accuracy and efficiency of spectral acquisition. For these reasons, it was considered the use of vibrational spectroscopic techniques such as Fourier-transform spectroscopy (FT-IR) in (1) in the External Reflectance (ER) mode, (2) Fiber Optics Reflectance Spectroscopy (FORS) in the near-infrared region (NIR). These techniques are readily available at the HERCULES laboratory for *in-situ* applications.

More than that, an issue that needs to be solved is the large number of samples to be analyzed in a short amount of time. Most ivory inspections involve bulk confiscations of ivory tusks and carvings, and this adds to the tediousness of the current procedures involved. Based on previous research that successfully combined NIR (Chaitae et al., 2021; Power et al., 2019), FT-Raman (Nocete et al., 2013; H. G. M. Edwards et al., 2006; Brody et al., 2001) albeit with limited success, and FT-IR, with chemometric methods, the proposed methodology will

integrate the spectroscopic analyses with chemometrics, i.e. Principal Component Analysis (PCA) and Partial Least Squares-Discriminant Analysis (PLS-DA). This addition can help test the robustness of the results and analyze large datasets with several variables to be considered.

Methodology

The research methodology integrated two different approaches: the art-historical and the technical-scientific approaches. Using this set of approaches one can complement the shortcomings of each method.
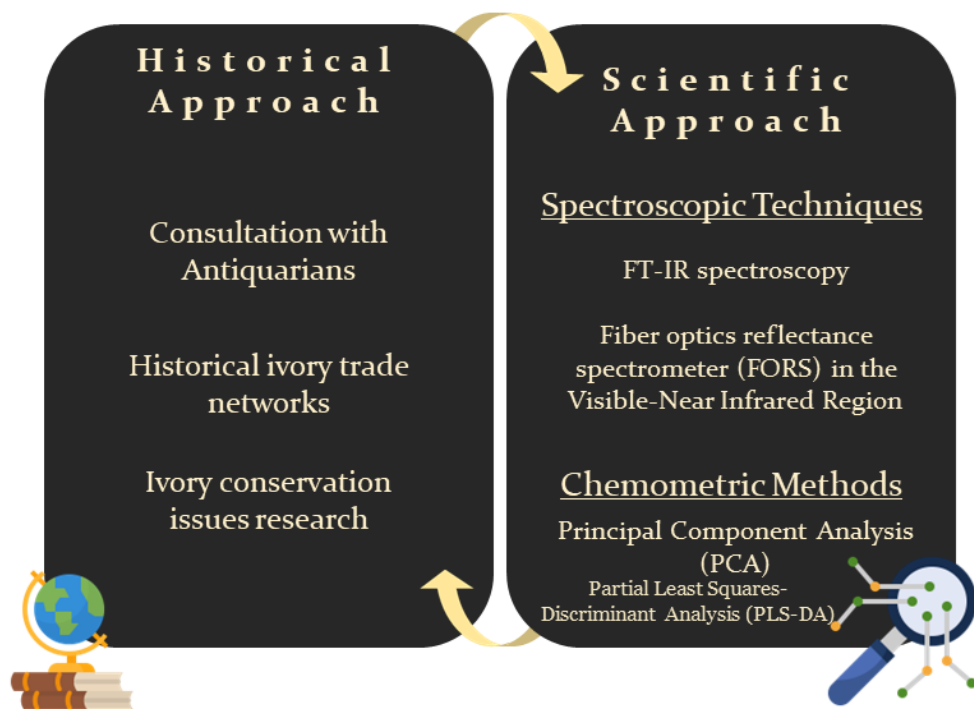
Ivories in Context: Historical Approach

Designating the provenance of the historic and contemporary ivory samples required the consultation of historical sources and seasoned antiquarians. Through laying out the historical context of the ivory trade and the relationship between ivory and the elephant, it sheds light at the various trade networks that allow for the probable designation of their provenance.

However, searching trade and historical sources can be tedious and the information that they provide can be limited. Moreover, most in-depth analyses require that portions of the samples be destroyed. This can be a problem for precious ivory artifacts. Thus, a complementary approach of nondestructive and non-invasive scientific analyses must be performed. This is where the scientific approach can be immensely helpful.

Ivories on the Field: Scientific Approach

The set of analytical techniques to be used was selected on the basis of the portability and availability of their instruments at the HERCULES Laboratory. Particularly, the methods utilized were Fourier-transform infrared spectrometry and fiber optics reflectance spectrometry (FORS) in the near-infrared region (NIR). The spectra were processed using chemometric methods of Principal Component Analysis (PCA) and Partial Least Squares-Discriminant Analysis (PLS-DA).

Samples

Data were collected from 72 ivory samples (n = 72) procured from organizations, museums, and personal collections. Most of the samples (28) were confiscated ivories with permission from the Instituto da Conservação da Natureza e das Florestas (ICNF) in accordance with the Convention on International Trade in Endangered Species of Wild Fauna and Flora (CITES). The African elephant tusk was gotten from Jardim Zoológico-Lisbon while the Asian elephant tusks were procured from Royal Kraal Elephant Village-Bangkok. The other samples were from the historic ivory collection of São Roque Antiguidades

e Galeria de Arte in Lisbon, Museu Nacional Arte de Antiga, and from the personal collections of renowned Antiquarians in Portugal.
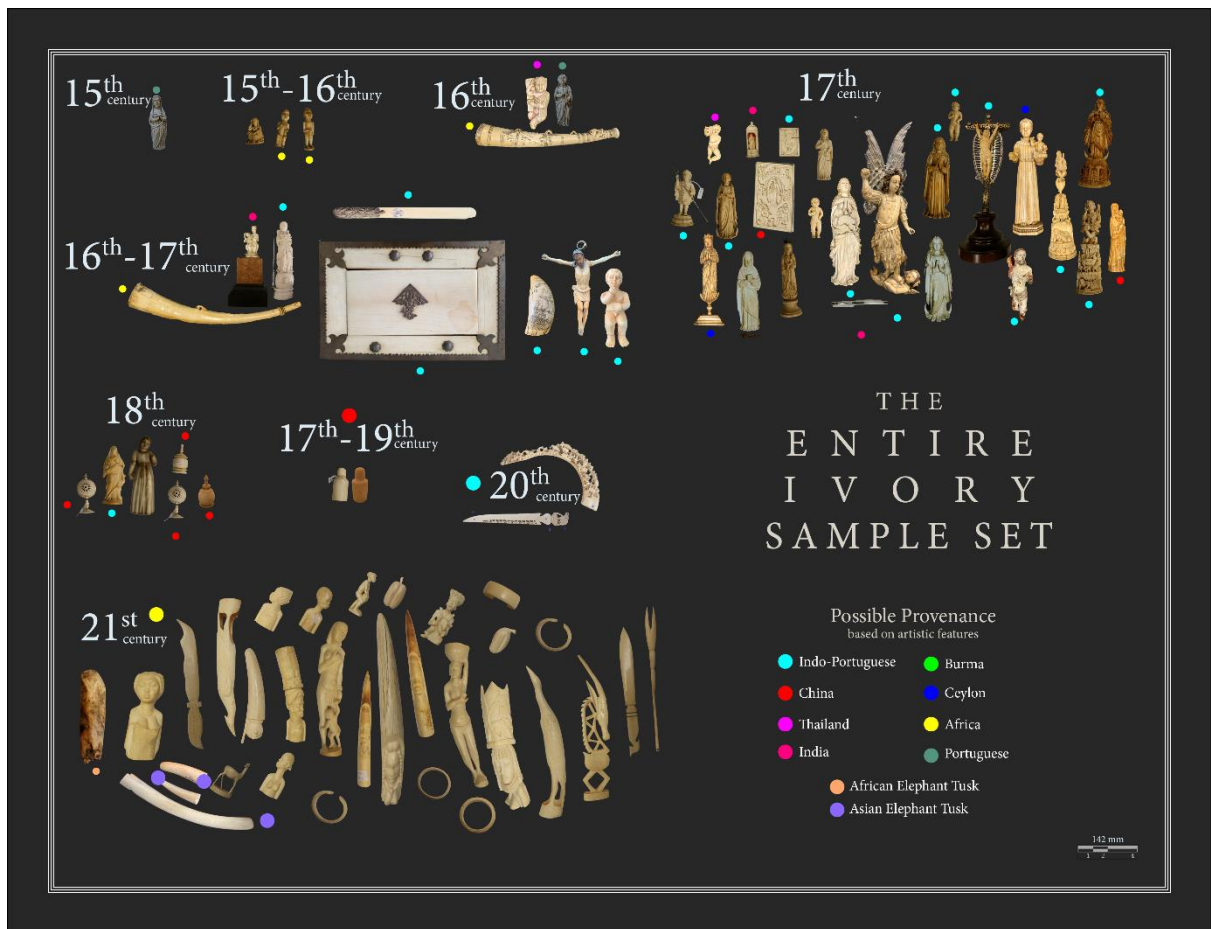
To simulate the situation of enforcement officers in field investigations, the ivory sources were heterogeneous. Because of this, the attempt of controlling some factors was beyond the scope of this research, including the characteristics of the host animals (e.g. sex, age) and storage conditions of the ivory (e.g. humidity, degradation processes). Some steps were taken to minimize their confounding effects, but this does not eradicate their effects completely. It is a trade-off that has to be taken in mind in the development of this methodology for field investigations.

Data Collection and Sampling

The ivory samples were prepared for analysis by wiping the surface with a tissue. Minimum sample preparation was undertaken to simulate the environment during investigations.

Sampling points were determined by the evenness of the surface for analysis. Flat surfaces were chosen to produce high-quality spectra. Triplicate measurements were performed at each sampling point, and up to five sampling points were chosen per ivory sample. Points of analysis were taken along the surfaces perpendicular and parallel to the main longitudinal axis of carvings and tusks.

Fourier-Transform Infrared (FT-IR) Spectrometry

The spectra were collected using the ALPHA FT-IR Spectrometer from Bruker Optics fitted with the External Reflectance module. The OPUS software was used for spectral measurements and data transformation.

Before each round of measurements, the gold standard is fitted through the opening. A round of startup tests was performed to ensure that the instrument was in good condition for analysis. After the startup tests, the signal was checked in the *Interferogram* tab. The amplitude is usually at least -8000 for the gold standard. Once the signal has stabilized, the peak position is saved (*Interferogram > Check Signal > Save Peak Position*). Then, a background measurement was performed and saved for a round of measurements. The gold standard is then replaced with a 3-mm collimator. The sample is placed approximately 1-2 mm in front of the collimator and the surface is ensured to be perpendicular to the beam as much as possible.

Pictures of the sampling points were acquired using the *video-assisted measurement* feature of the OPUS software before the actual measurement. Repeated measurements were performed with a 5-second delay between each round, with 128 scans at 4 cm^{-1} resolution. The spectra were acquired in reflectance mode and transformed into absorbance through the Kramers-Kronig Transformation in the OPUS software (*Manipulation > Kramers-Kronig Transformation > Absorbance*) The transformation was used to correct spectral distortions. Finally, these were processed into .dpp files for further data post-processing. See Appendix I for full instrument specifications.

Visible-Near Infrared NIR Fiber Optics Reflectance Spectrometry (Vis-NIR FORS)

The spectra were acquired using i-Spec® 25 from B&W Tek, a full-range broadband mobile spectrometer with a handheld reflectance probe for measurements across the Vis-NIR range from 400-2500 nm. Each of the detectors scans along a particular spectral range:

- BRC711U-512: 345.6 nm - 1061.3 nm
- BTC261P-512-OEM6: 883.0 nm - 1718.0 nm
- BTC263E-256-OEM6: 1482.4 nm - 2654.9 nm

An optimized set of options were selected:

Detector	Spectral Range
BRC711U-512	**345.6 nm - 1061.3 nm**
Integration time	50 ms
Average	25

Smoothing	None
BTC261P-512-OEM6	**883.0 nm - 1718.0 nm**
Integration time	224 µs
Average	50
Smoothing	None
Detector Mode	High Sensitivity
BTC263E-256-OEM6	**1482.4 nm - 2654.9 nm**
Integration time	300 µs
Average	100
Smoothing	None
Detector Mode	High Sensitivity

The instrument was calibrated for acquisition using a dark and white reference. This calibration procedure was done before the initial measurement and every 10 minutes of measurements. In every acquisition, the probe is positioned in such a way that the beam is as perpendicular as possible to the sample surface. Measurements are performed in triplicate. Using the iSpec® 4 software, the spectra were obtained in transmission mode and processed into .csv files. See Appendix I for full instrument specifications.

Chemometrics

The spectral data were processed using MATLAB with the PLS_Toolbox Add-on from Eigenvector Research, Inc. Data was then processed independently per instrument (FT-IR and FORS) and per wavelength region (Visible, IR, NIR).

Pretreatment of Savitsky-Golay 1ST Derivative, SNV, and Mean Center were then applied.

For analyzing the **FT-IR spectra**, only PCA was used. To build the PCA calibration model, only the models from ICNF and the Elephant Tusk, which are most probable to be African, were utilized. The rest of the samples are then projected. Based on the T2-statistic and Q-statistic it is possible to investigate the model fitting for all samples. Those that were below the confidence limit of 95% were close to the model center and are most probably African samples. Those above the confidence level are less likely or may not be African. Thresholds were imposed to the confidence limit to avoid making decisions on the overlap. Samples that are within the limit are to be designated as inconclusive (Figure 13).
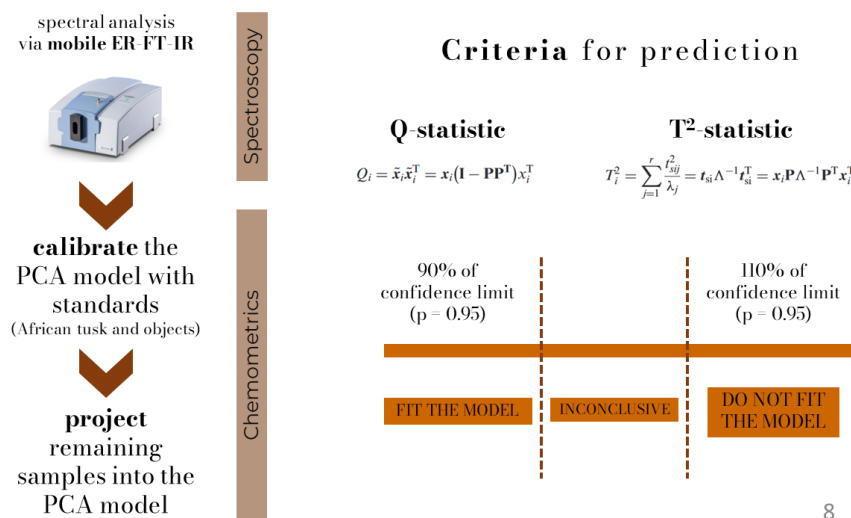
spectral analysis via **mobile ER-FT-IR**

Spectroscopy

Chemometrics

calibrate the PCA model with standards (African tusk and objects)

project remaining samples into the PCA model

Criteria for prediction

Q-statistic

$$Q_i = \tilde{x}_i \tilde{x}_i^T = x_i(I - PP^T)x_i^T$$

T²-statistic

$$T_i^2 = \sum_{j=1}^{r} \frac{t_{sij}^2}{\lambda_j} = t_{si}\Lambda^{-1}t_{si}^T = x_i P \Lambda^{-1} P^T x_i^T$$

90% of confidence limit (p = 0.95)

110% of confidence limit (p = 0.95)

FIT THE MODEL | INCONCLUSIVE | DO NOT FIT THE MODEL

8

Figure 13. Identification scheme for FT-IR analyses.

For analyzing the **FORS spectra in the NIR region,** both PCA and PLS-DA were utilized. The PCA analysis was used as an exploratory method, while PLS-DA was used as a classification method to discriminate Asian and African ivory. This method was also preferred as both African and Asian ivory were present as standards.

At first, the PLS-DA model was calibrated using the African and Asian tusk samples. Then, pseudo-labels were assigned to the rest of the samples. The calibrated model was used to predict the rest of the samples until all of them have been classified. The model was then cross-validated, and results were evaluated for suitability for on-field investigations.
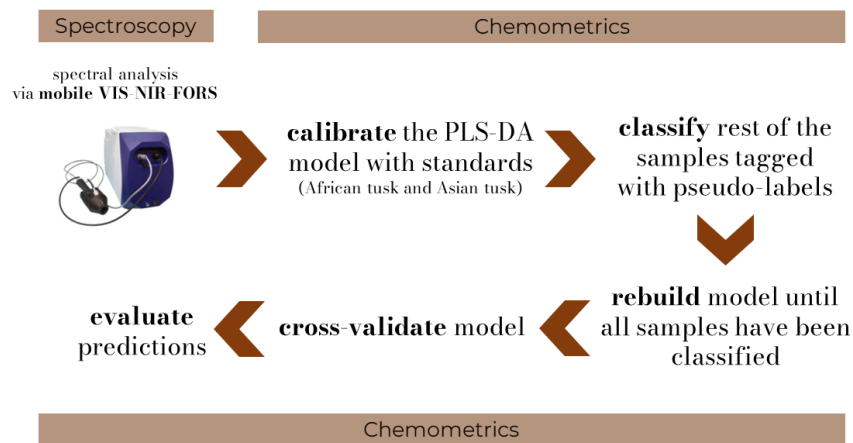
Figure 14. Classification scheme for FORS spectra in the near-infrared region (NIR).

Results and Discussion

Classifying African and Non-African Ivory using FT-IR Analysis

As a technique, FT-IR spectrometry enabled for discriminating African samples from those that are less likely to be African, around the molecular fingerprint region (1700 cm^{-1} to 500 cm^{-1}). Using Principal Component Analysis (PCA) with the Q-statistic and Hotelling's T^2 statistic as a criterion, it was possible to investigate which samples fit the calibrated model, and thus, are assumed to be of African origin. First, the PCA model was calibrated with the ivory carvings from ICNF and the African elephant tusk from *Jardim Zoológico de Lisboa*, as these samples have a high probability of being from the African elephant. Then, the remaining samples are projected into the model. Generally, the Q-statistic is more sensitive than the T^2 statistic—which means, since it is very small, any minor change in the system can be detected. Consequently, the Q-statistic reveals how well each sample conforms to the model, while the T^2-statistic explains the variation of each sample within the PCA model (Mujica et al. 2008). In this case, samples with a high Q-statistic indicate the presence of spectral features that are not commonly observed to that of the samples that fit the model. It is a measure of the difference or residual between each sample and its projection into the model's principal components. On the other hand, samples with a high T^2-statistic indicate that samples have the same spectral features as observed in the model, albeit different in intensity. Thus, both Q-statistics and T^2-statistics were considered in the criterion. If a sample has both Q-statistics and

T^2-statistics within 90% of the confidence limit at 95%, it means that it fits within the model and is thus considered to be African. Those that do not fit the model have both of these criteria beyond 110% of the confidence limit at 95%, and might not be of African origin. Samples within these limits are considered inconclusive. The classification of some samples can be seen in previous figures (Figure 3 and Figure 4).

The FT-IR spectrum of ivory is a combination of bands attributed to collagen, carbonated hydroxyapatite, and water (Figure 1). As observed, the most intense peak at 1045 cm^{-1} is associated with the υ_3 stretching of PO_4 in carbonated hydroxyapatite. The summary of vibrational bands are tabulated (Table 1).
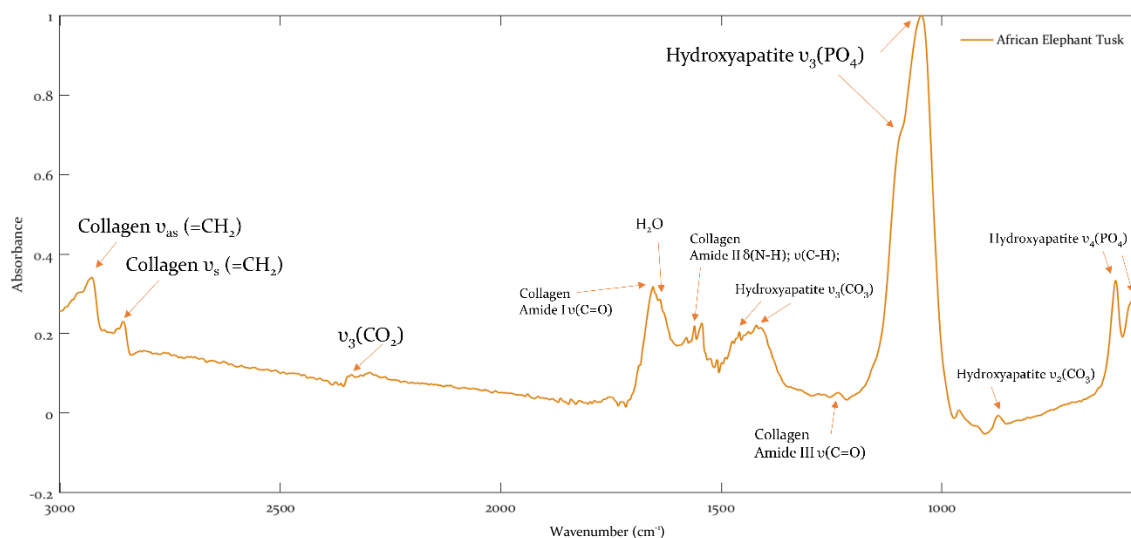
Figure 15. FT-IR spectrum of African elephant ivory. Vibrational assignments are designated.

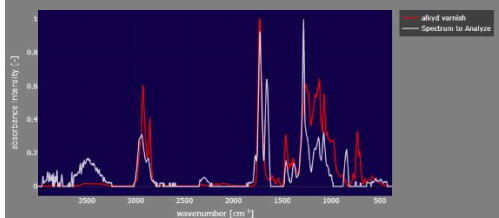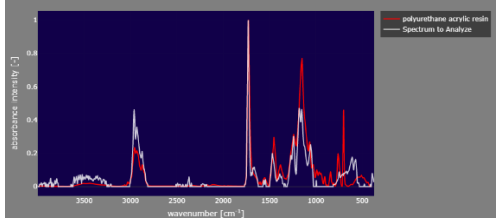*Table 3. Vibrational modes and their corresponding wavenumbers.*
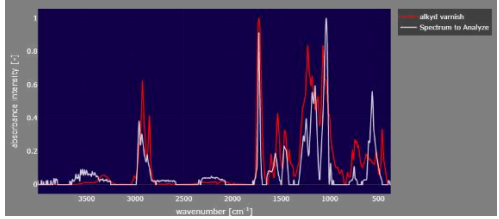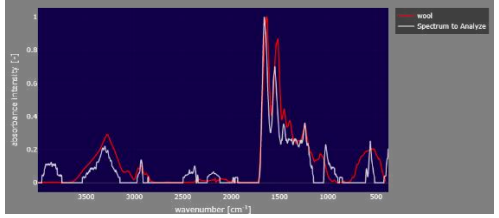
Wavenumber (cm^{-1})	Vibration Mode	Reference
2930 cm^{-1}	Collagen υ_{asym}(-CH$_2$)	Guennec (2020)
2850 cm^{-1}	Collagen υ_{sym}(-CH$_2$)	Guennec (2020)

2346 cm^{-1}	$\upsilon_3(CO_2)$	Guennec (2020)
1654 cm^{-1}	Collagen Amide I $\upsilon(-C-O)$	Payne and Veis (1988)
1630 cm^{-1}	H_2O	Sun et al. (2022)
1561 cm^{-1}	Collagen Amide II $\delta(N-H) + \upsilon(C-H)$	Payne and Veis (1988)
1554 cm^{-1}	Hydroxyapatite $\upsilon(-C-O)$	Sun et al. (2022)
1459 cm^{-1}	Hydroxyapatite $\upsilon_3(-CO_3)$	Sun et al. (2022)
1421 cm^{-1}	Hydroxyapatite $\upsilon_3(-CO_3)$	Wang et al. (2022)
1409 cm^{-1}	Hydroxyapatite $\upsilon_3(-CO_3) + \omega(-CH_3)$	Guennec (2020)
1245 cm^{-1}	Collagen Amide III $\delta(N-H) + \upsilon(C-N)$	Payne and Veis (1988)
1088 cm^{-1}	Hydroxyapatite $\upsilon_3(-PO_4)$	Wang et al. (2022)
1045 cm^{-1}	Hydroxyapatite $\upsilon_3(-PO_4)$	Rozalen and Ruiz Gutierrez (2015) ; Nocete et al. (2013)
960.3 cm^{-1}	Hydroxyapatite $\upsilon(-PO_4)$	Wang et al. (2022)
873 cm^{-1}	Hydroxyapatite $\upsilon_2(-CO_3)$	Wang et al. (2022)
871 cm^{-1}	Hydroxyapatite $\upsilon_2(-CO_3)$	Wang et al. (2022)
606 cm^{-1}	Hydroxyapatite $\upsilon_4(-PO_4)$	Wang et al. (2022)
567 cm^{-1}	Hydroxyapatite $\upsilon_4(-PO_4)$	Wang et al. (2022)

From the total amount of samples from this work analyzed using FT-IR (n = 55) a set presented different spectral features that were different from those of ivory. Based on the Q-statistic values, the following samples have been deemed anomalous (Table 2), which means that based on their spectra these might not be purely ivory. This can be due to lacquer, varnish, or other coatings applied to the samples, or that these are made of some organic resin. The corresponding spectra have been compared with those of an open-source reference library, OpenSpecy (Cowger et al. 2021). A notable observation is that sample BJ5, which was supposed to be a scrimshaw whale tooth, has been found to lack the

vibrational signatures associated with phosphate, carbonate, and amide bands. Based on its FT-IR spectrum it cannot be confirmed to be ivory. Additionally, a copy of the sample has been found to be sold in Etsy as scrimshaw faux whale tooth (Figure 2).

Table 4. Samples with unusually high Q-statistics that might not be ivory or combined with other coatings that might affect the corresponding analyses. Spectra in white correspond to the sample spectra and spectra in red correspond to the database spectra.

Anomalous Samples with High Q-statistics		
2529	With alkyd varnish	
2498	Polyurethane acrylic resin	
2488	With alkyd varnish	
BJ2	With traces of wool	

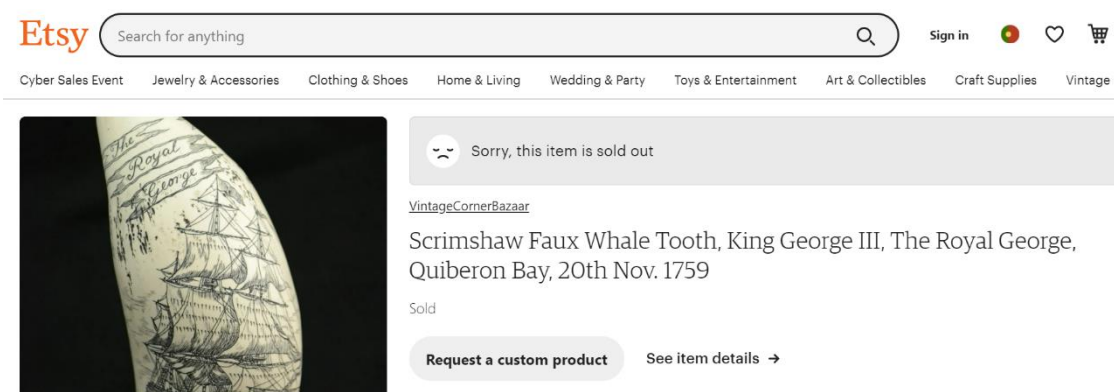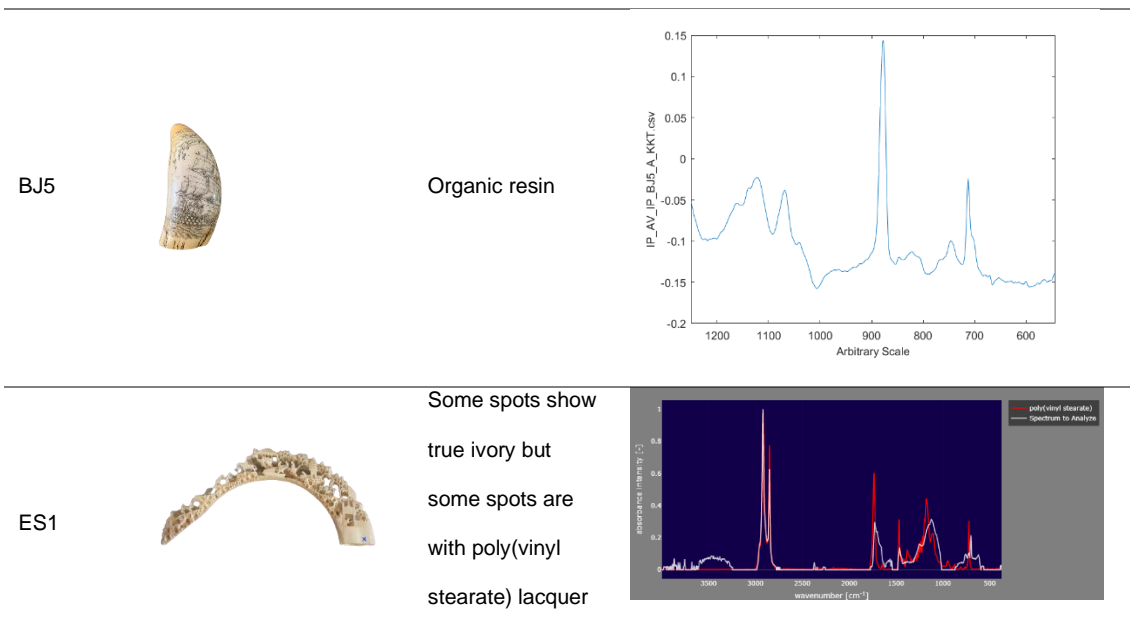|			
BJ5		Organic resin	
ES1		Some spots show true ivory but some spots are with poly(vinyl stearate) lacquer	

Figure 16. Screenshot of the Etsy sale page for faux whale tooth scrimshaw. Accessed 23/11/2022.

With the T^2- and Q-statistics plot (Figure 3) it is possible to investigate the model fitting for all samples. The plot is intersected by two lines that represent the Reduced Statistic Threshold (p=0.950) based on the calibrated model of ivory samples from ICNF and the African elephant tusk. To determine if the model fits the sample (FIT MODEL), both the T^2- and Q-statistics must be within 90% of the confidence limit at 95%, and for samples to be classified as not fitting the model (DO NOT FIT MODEL), both of those classification indices must be beyond 110& of the confidence limit at 95%. Samples within these limits are classified as

inconclusive. As observed, the samples that do not fit the model have high T^2- and Q-statistics and are clustered at the far upper right. On the other hand, the samples that fit the model cluster within the bottom left (Figure 3). Essentially the samples that fit the model were more likely to be of African origin, while the samples that do not fit the model are less likely to be African, which in this case is reasonable to assume is Asian.
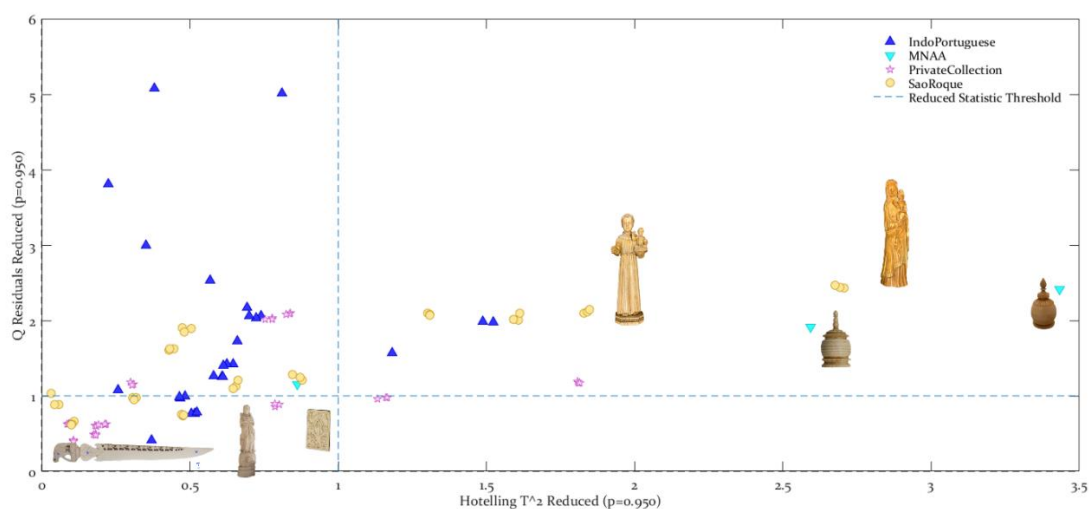

Figure 17. Q-statistics and T2-statistics plot with the samples projected based on the 95% confidence limit from the calibration samples (ICNF and AfricanTusk). Upper right corresponds to samples that do not fit with the calibrated model. Bottom left corresponds to samples that fit well with the model and are thus African ivory.

Based on past iterations of building the model, the region with the most variance was concentrated within the 1600 cm^{-1} and 600 cm^{-1} which also encapsulates the "molecular fingerprint" region in FT-IR. Hence, the final model was limited to this region to improve the variance captured by the principal components and to capture molecule-specific vibrational modes.

While the T^2- and Q-statistics are quantitative tools to determine the model fitting, the scores and loading plots (Figure 4) are more of qualitative tools to

describe how samples fit with the model. Samples that are nearer to the model center fit the model well and are thus more likely to be African ivory (Figure 4a). Samples that are farther and beyond the confidence limit lack the spectral features for their origin to be assumed of African ivory.

Based on the loading plots (Figure 4b and 4c), the first principal component (PC1) captured 48.60% of the total variance within the samples, while the second principal component (PC2) represented 18.57% of the total variance. The samples that do not fit the model diverge along the PC2 axis. Hence, the most significant wavenumbers can be determined by looking at PC2 (Figure 4b), which are 1034 cm^{-1} and the shoulder at 1109 cm^{-1} which are associated with the u_3 stretching of PO_4 in carbonated hydroxyapatite, while those at 596 cm^{-1} and 555 cm^{-1} represent the corresponding u_4 stretching. Based on these findings, the PCA model developed discriminates based on the distribution and concentration of hydroxyapatite in the ivory. There were contributions from the protein and collagen content, but these were not as significant as that of hydroxyapatite to actually discriminate between the two species.
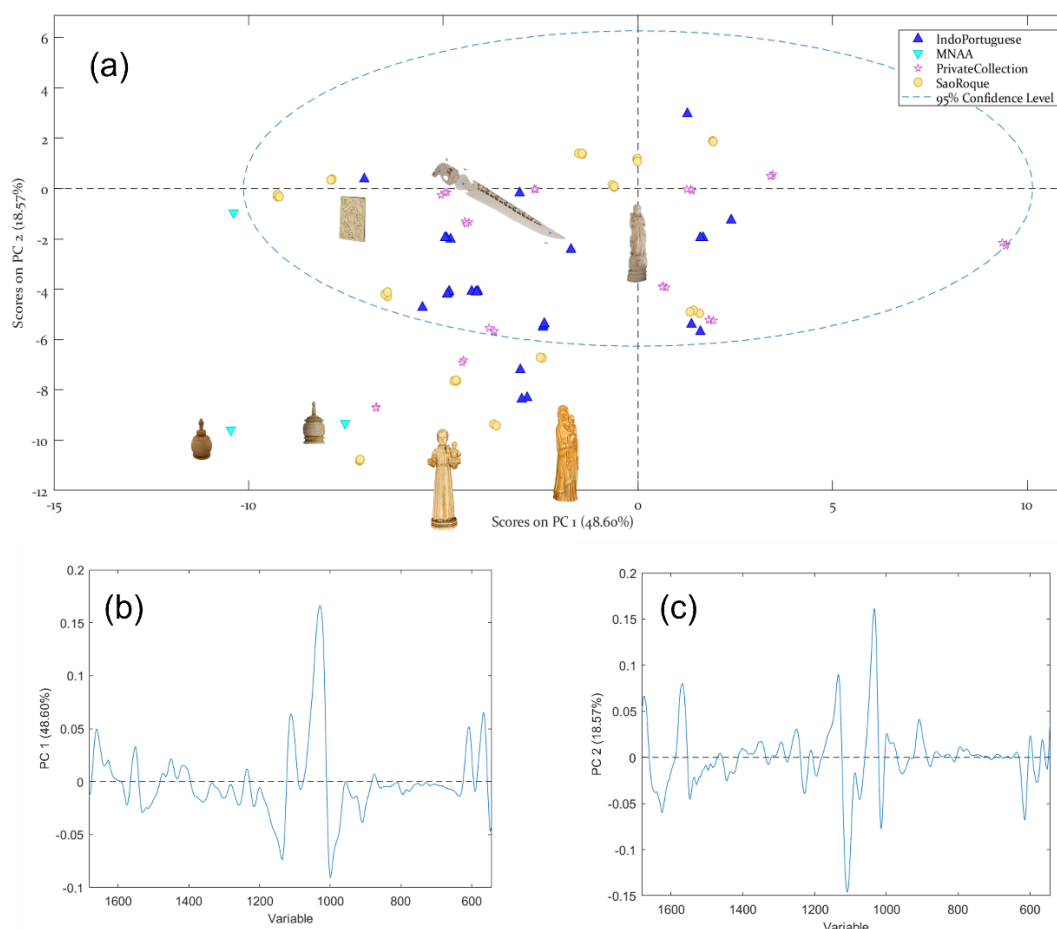
Figure 18. PCA score plot (a) with corresponding loading plots in PC1 (b) and PC2 (c). Notice how the samples that do not fit with the model are far from the model center.

To determine how African-classified samples were different from those that are not African, the samples that did not fit with the model were investigated based on their T^2 contributions (Table 3). The significant T^2 contributions came from wavenumbers associated with the carbonate and phosphate groups of carbonated hydroxyapatite, and some from the amide I band of collagen. Their absorbance spectra and first derivative spectra were plotted (Figure 5) with the calibration samples (ICNF and African elephant tusk) in green and dark green, while the samples that did not fit the model are in yellow and blue.

In agreement with the T^2 contributions, the African and not African samples diverged in wavenumbers that are associated with the υ_3 stretching of PO_4 in

hydroxyapatite at 1030 and 1100 cm^{-1}. Samples that are not of African origin had their most intense peaks at 1035 cm^{-1} shifted to higher wavenumbers, with the shoulder band at 1096 cm^{-1} at higher absorbance intensities. For those samples classified as African, the corresponding shoulder band were shifted at lower absorbance intensities, making the shoulder band more pronounced, and for those that were not classified as African, a smooth slope (Figure 5, encircled). On the other hand, the bands at 568 cm^{-1} associated with υ$_4$ stretching of PO$_4$ in carbonated hydroxyapatite exhibit a lesser absorbance intensity for the not African samples. Additionally, for the same samples, the bands at 1657 cm^{-1} associated with the amide I band of collagen also revealed lower absorbance intensities.

Table 5. Significant T^2 contributions from samples that do not fit the model, to aid in determining which wavenumbers they diverge from the calibrated model.

| Significant T^2 Contributions from Samples that Do NOT fit the Model		
Wavelength (cm^{-1})	**Vibration Mode**	**Reference**
1030 cm^{-1}	Hydroxyapatite υ3(-PO$_4$)	Rozalen and Ruiz Gutierrez (2015) ; Nocete et al. (2013)
1110 cm^{-1}	Shoulder associated with vibration of Hydroxyapatite υ$_3$(-PO$_4$) at 1088-1096 cm^{-1}	Wang et al. (2022)
568 cm^{-1}	Hydroxyapatite υ$_4$(-PO$_4$)	Wang et al. (2022)
1657 cm^{-1}	Collagen Amide I υ(-C-O)	Payne and Vais (1988)
1551 cm^{-1}	Hydroxyapatite υ(-C-O)	Sun et al. (2022)
608 cm^{-1}	Hydroxyapatite υ$_4$(-PO$_4$)	Wang et al. (2022)
2928 cm^{-1}	Collagen υ$_{as}$(-CH$_2$)	Guennec (2020)
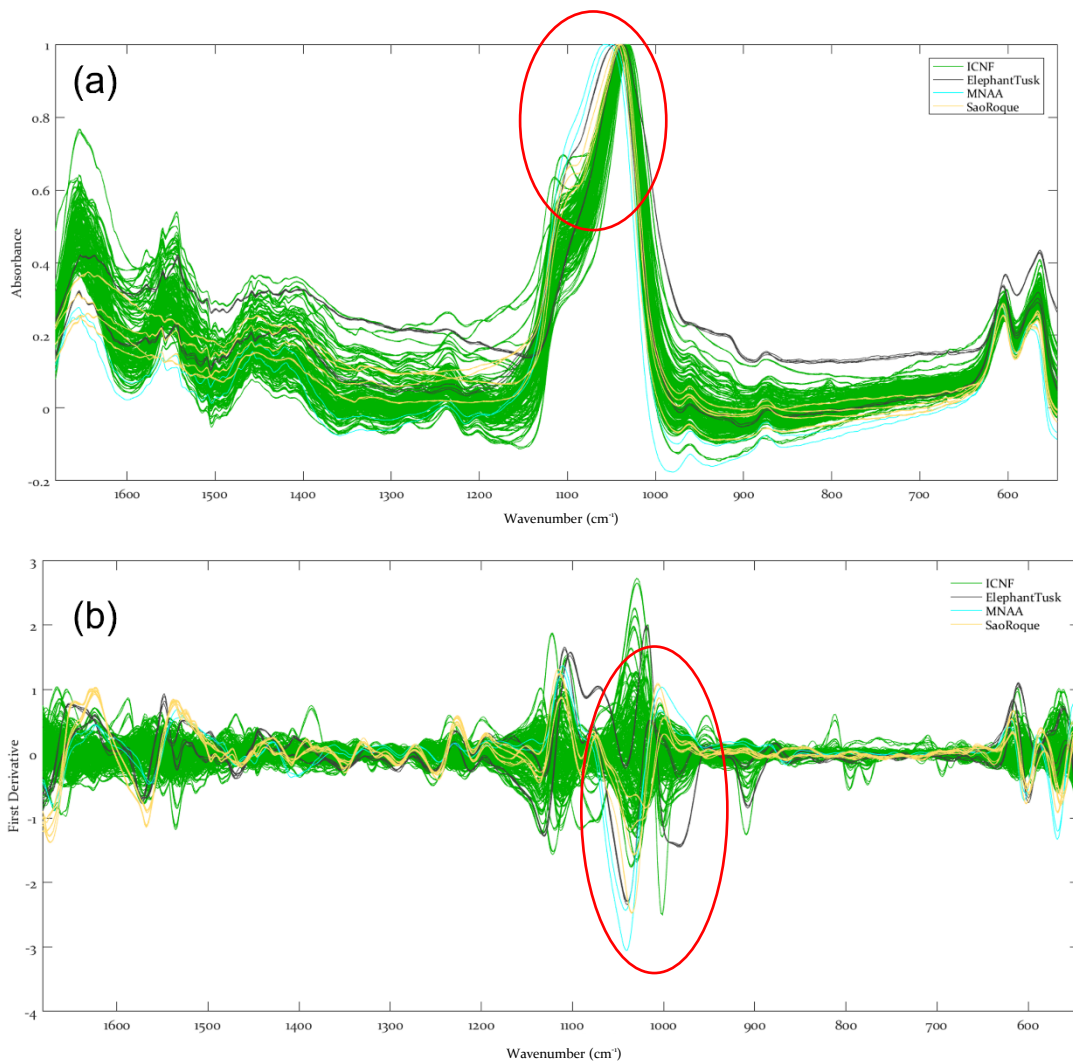
Figure 19. Raw data (a) and first derivative (b) plots of calibrated samples (ICNF and ElephantTusk) and test samples NOT fitting with the model to highlight the diverging intensities at wavenumbers with high T^2 contributions.

To understand how FT-IR can be used to discriminate between ivory species, it is necessary to understand ivory composition. Ivory is composed of nanocrystals of carbonated hydroxyapatite in a collagen matrix. Recent studies (Albéric et al. 2018) have described the three-dimensional structure as mineralized collagen fibers (MCF). The main component of the inorganic phase is called dahlite, which is $Ca_{10}(PO_4)_6(CO_3) \cdot H_2O$ (McConnell 1965). The rest are composed of small amounts of calcium carbonate and calcium fluoride.

Conversely, majority of the organic component is Type I collagen, which contains a high proportion of the amino acids—glycine, proline, and hydroxyproline. Non-collagenous proteins, lipids, and mucopolysaccharides comprise the remainder (Godfrey et al. 2002). Geochemical factors affect ivory composition across various habitats. For instance, dietary factors linked to external sources of vitamin C could influence the composition of collagen, while drinking water affects the mineral phase (Raubenheimer et al. 1998). Geographic variations in nutrient sources and climatic changes could also affect the size of carbonated hydroxyapatite crystals and the overall composition of collagen. For example, the size of hydroxyapatite crystals were found to be smaller in Asian ivory than in African ivory (Nocete et al. 2013). As such, it is possible to discriminate between Asian and African ivory based on the characteristics of their organic and inorganic components. For instance, in fresh African elephant ivory, the ratio of inorganic to organic matter was found to be 65:35 (Webster, 1958). In fact, the FT-IR spectrum of ivory consists of absorption bands related to the vibrational modes of amide bands in collagen, phosphate and carbonate groups in carbonated hydroxyapatite, and water (Figure 1 and Table 1). Several studies have differentiated subspecies of African ivory based on the CO_2 molecule within the inorganic crystal matrix (Guennec 2020) and species of African and Asian ivory based on the characteristics of the band related to phosphate in hydroxyapatite (Nocete et al. 2013).

In this investigation, the difference between African and non-African elephant ivory (which, in this case, is reasonable to assume that is Asian) was found to be related significantly to the peak and shoulder bands associated with the u_3 stretching of the phosphate group in carbonated hydroxyapatite. Based on

the T^2 contributions, absorbance spectra, and first derivative from the non-African samples, it was revealed that the most intense peak at 1045 cm^{-1} have shifted to higher wavenumbers in the non-African samples. Additionally, the shoulder band at 1088 cm^{-1} also has a higher absorbance value in non-African samples in comparison with the African samples (Figure 5). What can possibly explain this deviation is a natural phenomenon called carbonate substitution. In biological apatites, carbonate ions can be incorporated to the crystal lattice rather than existing as adsorbed, discrete mixtures of carbonate phases (LeGeros et al. 1969). Since ivory is a porous material, exchange and deposition of various ions and minerals within the lattice is promoted. The main inorganic component of ivory, hydroxyapatite, can undergo alterations such as anionic exchange with fluorine, cationic exchange with strontium, radium, and lead, and substitution of phosphate groups with carbonate (O'Connor 1984). Two types of substitution have been known to occur in bone and other biological calcified materials—where carbonate substitutes for phosphate (B-type substitution) and for hydroxide (A-type substitution). In mammoth and elephant ivory, mixed types of substitutions can occur (Sun, He, and Wu 2022). Since the most significant contribution in this investigation comes from the phosphate moiety, B-type substitution is of interest. This is relevant to the two most significant results in this investigation. First, the shift to higher wavenumbers of the most intense peak (1045 cm^{-1}) related to the phosphate moiety for the non-African samples can indicate a higher frequency of radiation required for the vibrational mode to be activated than in the African samples. This might imply that the crystal lattice is more ordered in the local sites related to the phosphate moiety, and thus relate to a higher degree of crystallinity. Its implication to macroscopic properties is that the non-African samples

(assumed to be Asian) can have stronger mechanical properties, i.e. stiffer and harder, compared with the African samples. Second, there were higher absorbance intensities observed with the non-African samples with the shoulder band at 1088 cm^{-1} as compared with the African samples. This might indicate lesser substitution of CO_3 with PO_4 in sites of non-African samples. The incorporation of the CO_3 within the hydroxyapatite lattice has proved to be disruptive in the A-site (phosphate) in a study by Madupalli et. al (2017). If there is less substitution of CO_3 in phosphate sites, this implies that the crystal lattice in non-African samples is more compact, and thus is related again to higher stiffness and hardness, as compared to African samples. In fact, a study by Wingender et. Al (2021) revealed that increasing carbonate content in hydroxyapatite has been linked to decreasing elastic moduli, likely as a result of decreased bond strength due to CO_3 substitution and Ca^{2+} loss (Wingender et al. 2021). In the same study, less crystallite size has also been postulated to cause the decrease in elastic modulus, i.e. a tougher, more elastic material. The two most significant results in this investigation complement each other based on their FT-IR spectra. African samples might appear to be softer and tougher in comparison with non-African samples (which can be reasonably assumed as Asian) based on their lesser degree of crystallinity due to more carbonate substitution, which might prove disruptive to the hydroxyapatite lattice structure. Significantly, ivory from Africa, particularly East Africa, is preferred by craftsmen since it is easily cut and worked (Walker 2010). Various elephant species produce ivory that can be categorized based on their "carvability"—as either "soft" or "hard". Ivory coming from both species of the African elephant is considered

softer than the Asian elephant ivory, which is the hardest and stiffest (Chaiklin 2010).

While some samples were classified as either African or non-African, the rest were considered inconclusive. This might be explained by the variation of chemical composition from the outer part of the tusk to the inner part (Chaitae et al. 2022), especially when the ivory objects were heterogeneous. The orientation of mineralized collagen fibrils, which are hypothesized to be related to the Schreger pattern, has also been found to vary across the tusk (Albéric et al. 2018). While FT-IR spectrometry provides an initial molecular blueprint of ivory, variation of the inorganic and organic components across various regions in the tusk proved to be an issue. Chaitae et. al (2022) suggests using the longitudinal section in analyzing tusks, while the cross-section proves to be more useful for ivory objects.

Aside from considering which sections are to be analyzed, complementary techniques must be performed to confirm possible mechanical implications of crystallographic properties of ivory. X-ray crystallography can prove useful to characterizing the crystallographic character of hydroxyapatite crystals, while mass analyses can confirm the ratio of Ca to P in Asian and African ivory. Nevertheless, for in-situ investigations, there is potential for FT-IR spectrometry to distinguish objects of African origin.

Discriminating Asian and African Ivory using FORS in the NIR

In this investigation, NIR spectrometry combined with chemometric methods like PCA and PLS-DA enabled for the classification of all ivory object samples as Asian-origin or African-origin. The use of FORS in the NIR (near infrared) region has proved itself useful as a nondestructive technique that is applicable to ivory objects of historic interest. Additionally, the minimal sample preparation required and its easy integration into processes is ideal for on-field investigations of confiscated ivories. However, its two significant downsides are broad and undefined spectral features and the contribution of scatter effects. This can be a result of multiple variables that must be considered for a more comprehensive understanding of what is happening in the system. Therefore, it is best to combine NIR with chemometric methods like PCA and PLS-DA—also known as multivariate spectral analysis. An NIR spectrum is essentially composed of overlapping absorption bands associated with overtones and combinations of vibrational modes like C—H, N—H, and O—H chemical bonds (Workman and Weyer 2008, 11).

Using Principal Component Analysis (PCA) as an exploratory method, all samples were projected into the model (Figure 6).
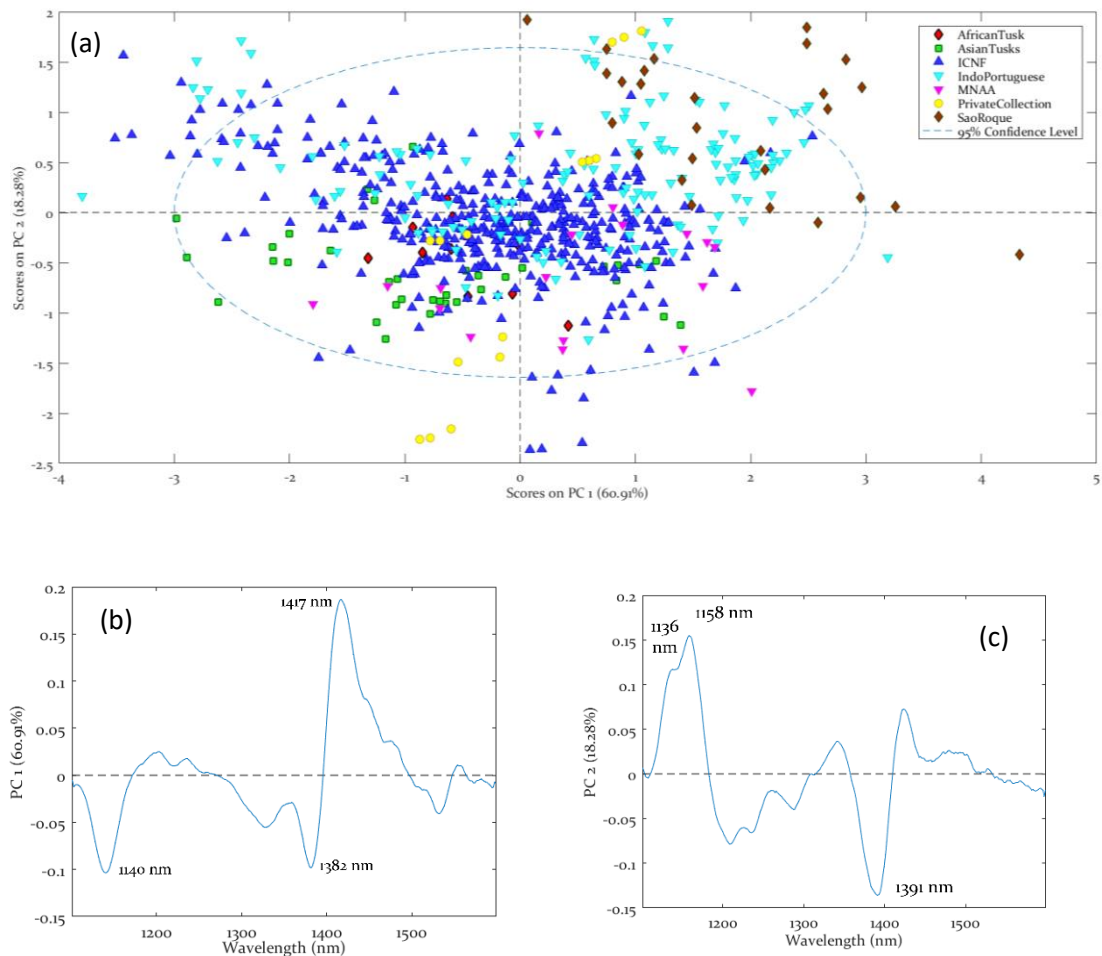
Figure 20. (a) Score plot for the entirety of samples, with 3 PCs, and corresponding loading plots for (b) PC1 and (c) PC2.

The first principal component (PC1) captured 60.91% of the variance within the dataset, while the second principal component (PC2) represented 18.28% of the total variance. Both components accounted for a total variance of 79.19% in the whole dataset. From the scores plot (Figure 6a), the *Indo-Portuguese* samples are distributed among clusters of samples—with the *São Roque* samples, and with the ICNF. Mots African Tusk samples cluster with the ICNF. Separation among these clusters is best explained by PC1 with significant variation at wavelengths 1140 nm, 1382 nm, and 1417 nm (Figure 6b). Overall, there is a separation among clusters, but classification of most samples remained inconclusive. Hence, a classification method—Partial Least Squares-Discriminant Analysis (PLS-DA)—was employed (Figure 7).
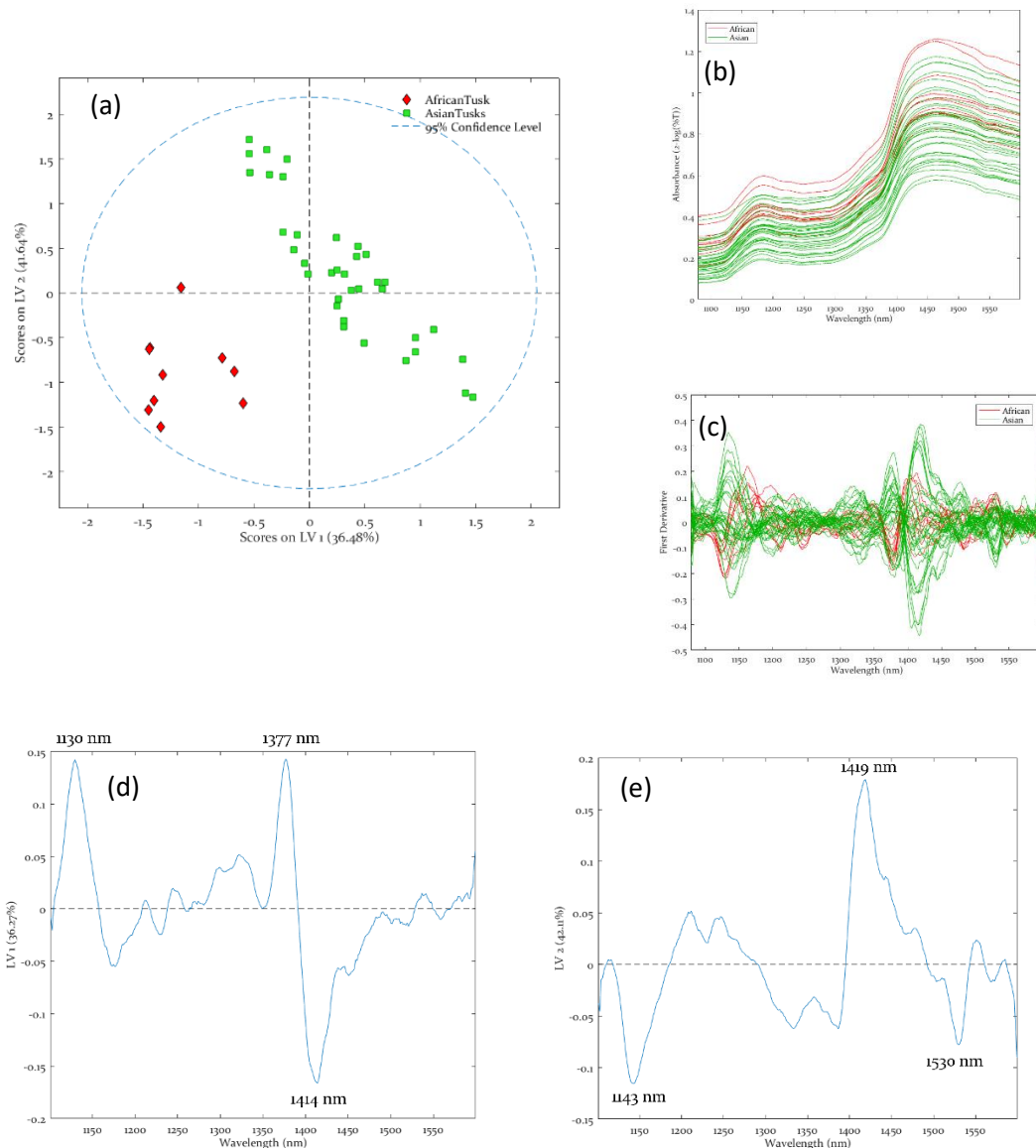
Figure 21. (a) Scores plot of the LV1 and LV2 illustrating the clustering of Asian and African Tusk samples, used for calibration. (b) Absorbance spectra of calibration samples. Notice how the African samples have higher absorbance values. (c) Preprocessed spectra in the first derivative. (d) Loading plot of LV1 with positive correlations at 1130 nm and 1377 nm, and a negative correlation at 1414 nm. (e) Loading plot of LV2 with positive correlations at 1419 nm, and negative correlations at 1143 nm and 1530 nm.

The PLS-DA model was calibrated with the tusk samples from Asian elephants (Royal Elephant Kraal Village—Thailand) and African elephants (Jardim Zoológico de Lisboa—Portugal) (Figure 7a). Although majority of the variance is captured by LV2 at 42.11%, the clusters are more well-separated along LV1, with a variance of 36.27% (Figure 7d and 7e). The most significant variables (wavelengths) that capture the variance along LV1 are at 1130 nm (C—

H vibrations related to collagen), and at 1377 nm and 1414 nm (O—H vibrations attributed to structural water molecules). Asian tusks exhibit a more dramatic change in slope along these wavelengths compared to African tusk samples (Figure 7b and 7c).
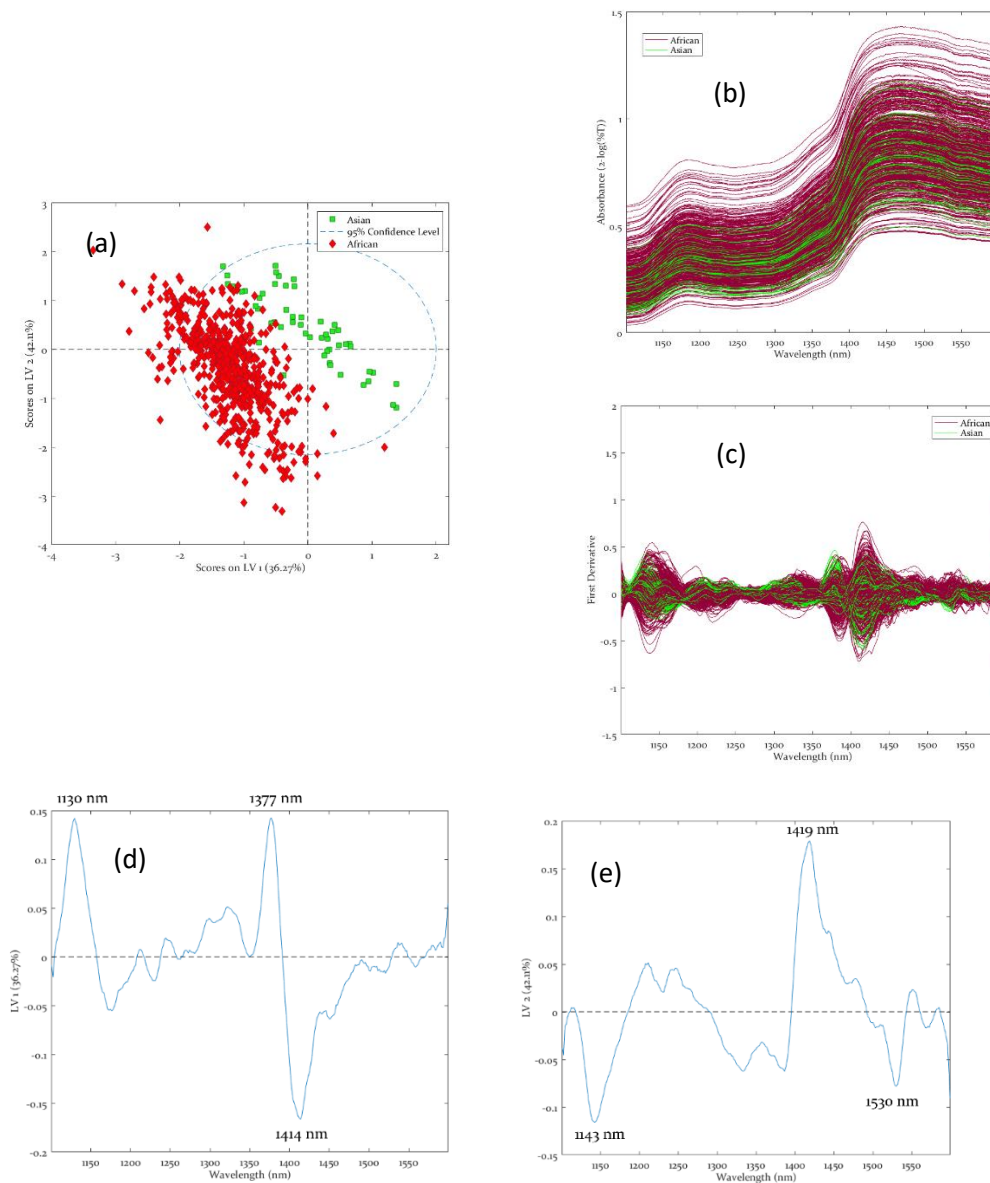
Figure 22. (a) Scores plot for LV1 and LV2, (b) Absorbance and (c) Preprocessed spectra in the first derivative for all the test samples including the calibrated samples, and (d and e) Loading plots from the calibration samples.

To apply the calibrated model to predict the rest of the unidentified samples as Asian or African, pseudo-labels were assigned to the samples to be predicted. Several iterations of the model were performed until all samples were classified

with the highest True Prediction Rate and lowest Misclassification Error for both Asian and African classes. The resulting assigned samples are displayed in the scores plot along with the samples used for calibration (Figure 8a to 8c). The loading plots based on the calibration samples display the exact wavelengths that were influential in assigning the rest of the unidentified samples as African or Asian (Figure 8d and 8e).

One of the initial plots that aid in visualizing the assigned samples is Class Pred Strict, where it displays the resulting samples that were assigned based on the calibrated model (Figure 9).
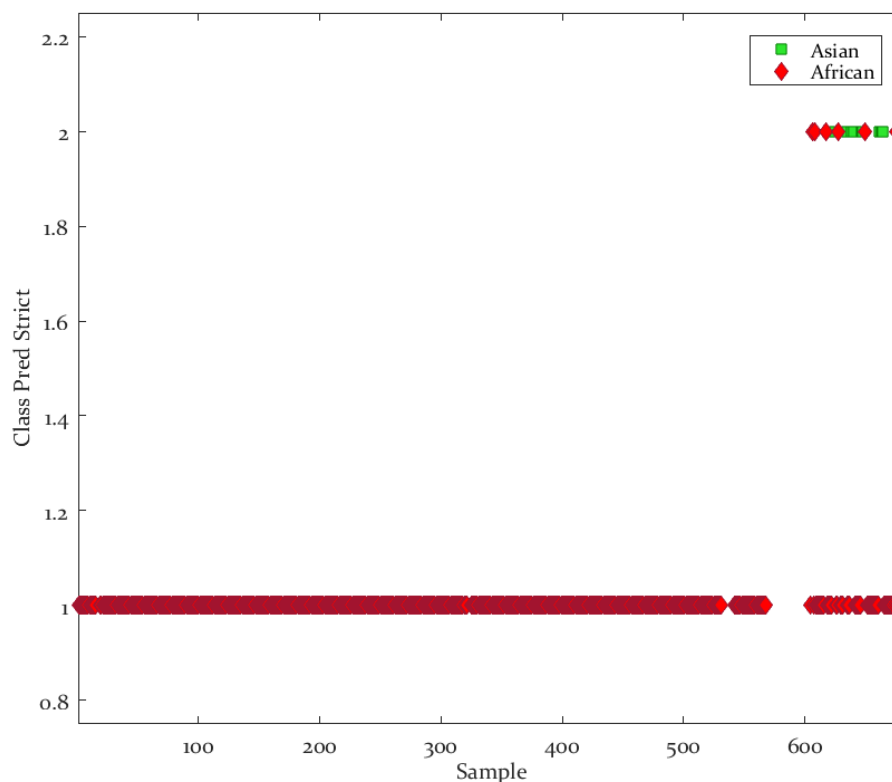
Figure 23. Class Pred Strict, displaying the samples that were assigned based on the calibrated model.

Samples are assigned a binary integer to which their spectra most identified with—in this case, 1 represents the samples assigned as African and 2 for the Asian ones.

While the Class Pred Strict plot (Figure 9) shows the samples as either African or Asian, the Class Pred Probability plots show the probability of the samples being African (Figure 10a) or Asian (Figure 10b). Notice how the plots are symmetrical to each other. For instance, in the plot showing the probability of each sample being African (Figure 10a), the higher the probability value of a sample is, it is more likely for the sample to be of African origin. The cut-off threshold for the probability is 0.6, and beyond that, the model classifies the sample as the specified class.
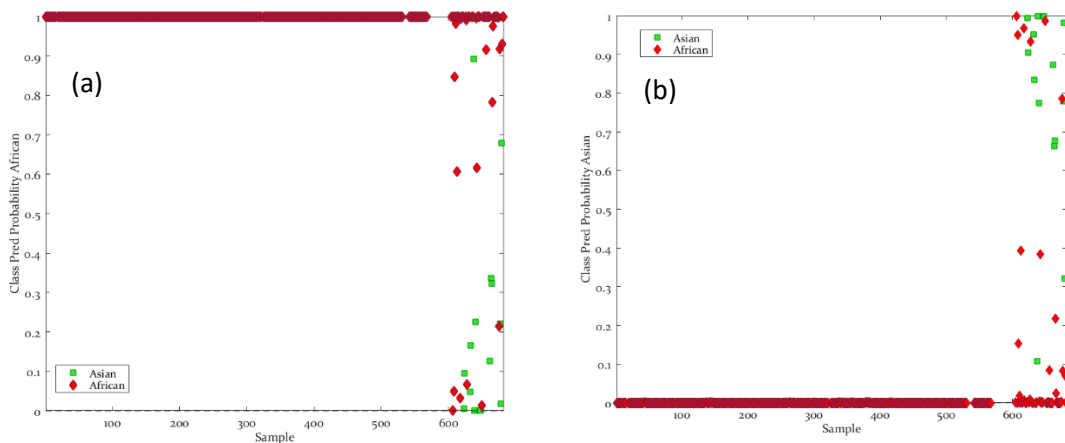
Figure 24. Probability plots for (a) African and (b) Asian samples. The threshold for classification is 0.6.

As observed in the previous plots, some Asian samples were being predicted as Asian, and vice versa. The Misclassified plot (Figure 11) provides a better visualization of these "misassigned" samples. Six African-assigned duplicates of samples were classified as Asian (red points along y = 1) while four (4) Asian-assigned duplicates of samples were misassigned by the model as African (green points along y = 0).
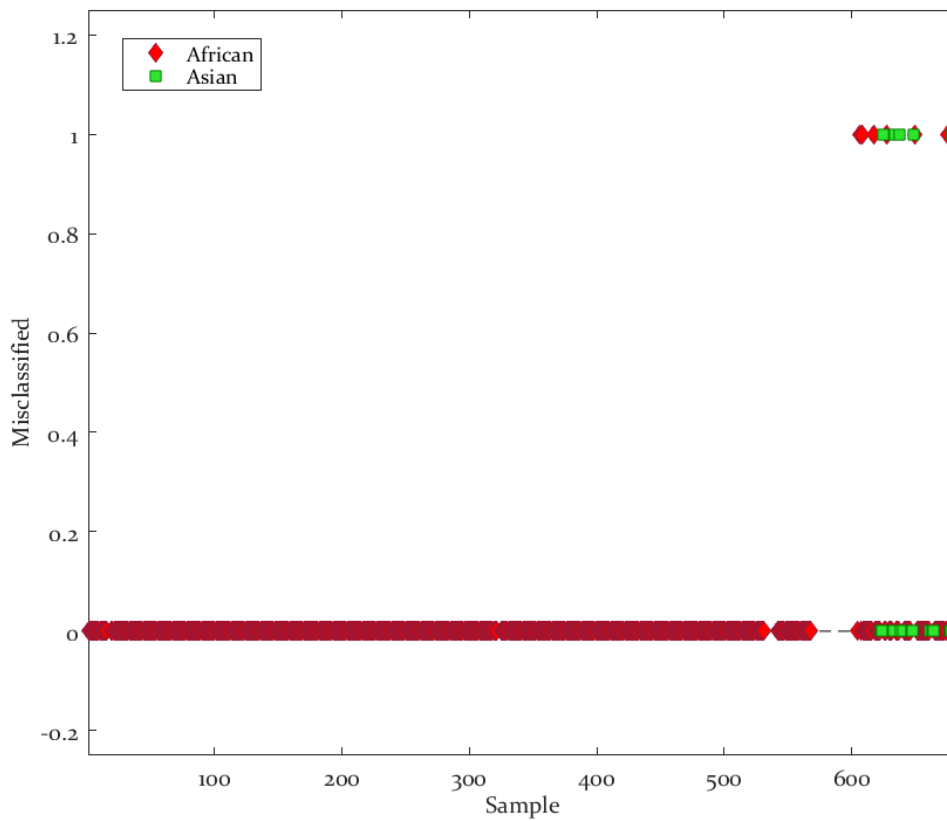
Figure 25. Misclassified samples with a value of 1 for samples assigned as Asian and value of 0 for samples assigned as African.

Some wavelengths are more influential than the others in predicting the samples. The most useful metric to measure the influence of a variable in prediction is the Variable Importance in Projection (VIP) score. The VIP scores plot illustrates this (Figure 12).
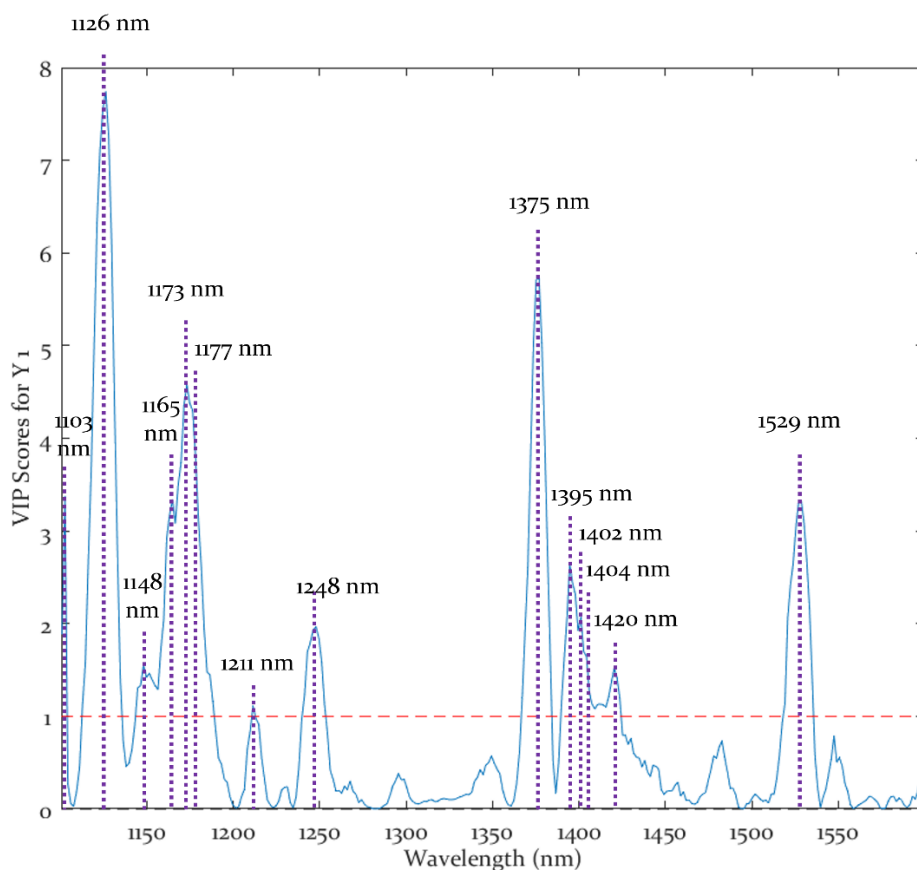
Figure 26. The Variable Importance in Projection (VIP) plot shows which wavelengths are significant in predicting the samples.

Variables, or wavelengths in this case, which have a VIP score higher than 1, are considered significant. The significant wavelengths and their corresponding vibrational modes were tabulated (Table 4). Most of these wavelengths are related to absorption bands caused by the vibrations of C—H and N—H in collagen, and O—H in structural water molecules.

Table 6. Wavelengths that are most significant in class prediction with their corresponding vibrational modes.

Wavelength (nm)	Vibration Mode	Reference
1126 nm	3υ C—H	Workman and Weyer (2008, 131)
1375 nm	$\upsilon_{asym} + \upsilon_{sym}$ O—H	Kolmas et al. (2015)
1173 nm	3υ C—H	Workman and Weyer (2008, 131)
1177 nm	3υ C—H	Workman and Weyer (2008, 131)
1529 nm	2υ N—H	Workman and Weyer (2008, 276)
1165 nm	3υ C—H	Workman and Weyer (2008, 131)
1395 nm	$\upsilon_{asym} + \upsilon_{sym}$ O—H	Kolmas et al. (2015)
1401 nm	$\upsilon_{asym} + \upsilon_{sym}$ O—H	Kolmas et al. (2015)
1404 nm	$\upsilon_{asym} + \upsilon_{sym}$ O—H	Kolmas et al. (2015)
1420 nm	$\upsilon_{asym} + \upsilon_{sym}$ O—H	Kolmas et al. (2015)
1248 nm	3υ C—H	Workman and Weyer (2008, 131)
1148 nm	3υ C—H	Workman and Weyer (2008, 131)
1211 nm	3υ C—H	Workman and Weyer (2008, 131)

The sensitivity and specificity of the developed PLS-DA model can be assessed using the True Prediction Rate (TPR), True Negative Rate (TNR) (Table 5), and Confusion Matrix (Table 6). Out of 612 spectral samples for the African class, 606 were classified correctly, resulting in a TPR of 99.020%. For the Asian class, 11 out of 15 spectral samples were classified correctly as Asian, resulting in a TPR of 73.333%. If the model were to be used in routine inspections, a misclassification error of 1.595% is within the acceptable range.

Table 7. Calibration and Prediction results for building the PLS-DA model for classification of ivory objects as African or Asian elephant origin.

	True Prediction Rate (Sensitivity)	True Negative Rate (Specificity)	N	Misclassification Error (Err)
Calibration Results				
African	100.00%	100.00%	10	0.0000%
Asian	100.00%	100.00%	36	0.0000%
Prediction Results				
African	99.020%	73.333%	612	1.595%
Asian	73.333%	99.020%	15	1.595%

Table 8. Confusion matrix for calibrated model.

	Actual Class	
	African	**Asian**
Predicted as African	606	4
Predicted as Asian	6	11

In cross-validating the PLS-DA model, samples from each class were randomly divided into calibration and validation datasets, with 20% of samples from each class. The TPR ranged from 93.028% to 99.020% for African samples, and for the Asian class, ranged from 93.333% to 100.000% (Table 7).

Table 9. Cross-validation results for developed PLS-DA model.

	Validation Results			
	True Prediction Rate (Sensitivity)	True Negative Rate (Specificity)	N	Misclassification Error (Err)
African	93.028% - 99.020%	93.333% - 100.000%	20% of $N_{African}$	3.248% - 6.962%
Asian	93.333% - 100.000%	93.028% - 96.591%	20% of N_{Asian}	3.248% - 6.962%

Considering the protein and collagen content, most significant contributions to class prediction arose from absorption bands related to C—H vibrations and N—H vibrations in collagen. In terms of composition, more than one-third of collagen composition is composed of glycine, while the rest are mainly proline and hydroxyproline. To convert proline residues to hydroxyproline in a reaction catalyzed by prolyl hydroxylase, ascorbic acid or vitamin C is required. Hence, collagen development relies heavily on the availability of vitamin C in the body. Browsers in the wild tend to consume more iron-chelating tannins in their diet, which is also generally low in vitamin C and iron (Clauss and Paglia 2012). African elephants living in arid areas showed significantly lower proline and hydroxyproline content and under-hydroxylation of lysine residues (Raubenheimer et al. 1998), which may be attributed to the lack of nutrients, particularly vitamin C, compared to those living in the well-forested areas. Arid regions also contain less water for drinking by animals. Hence, protein and water content may be less available for African elephants that originate from arid areas. While both species of African elephant inhabit both savannah and forests, Asian

elephants are mostly forest-(and grassland) dwellers (Choudhury 1999), where there is apparent availability of food and water. Ultimately, the variations of protein, collagen, and water content among various elephant species have agreed with the combined NIR and chemometric studies of Power et. al (2018) in distinguishing mammalian and avian bones, and more recently, of Chaitae et. al (2021) in distinguishing African ivory from those of wild and domesticated Asian elephants. However, issues in detection involved variation of protein and water across the sections, and further investigation must be undertaken on the effects of age, mechanisms of deterioration, and even subspecies level of African elephants that may be significant in building future models.

Summary of Classifications

In the following table (Table 8), summarized are the classification results of each sample from the techniques and their assigned artistic provenance. Results from a previous study (Parungao et al. 2022) utilizing Raman spectroscopy are also integrated to provide comparison. Samples with varying classifications among the vibrational spectroscopic techniques can be explained by several factors: variations of physical and chemical composition across the tusk, the contribution of relevant functional groups which are significant in each technique and minimized in the other, and other impurities like lacquers and coatings which may significantly introduce absorption bands that may interfere with modelling.

As observed in the summary table, few samples have an artistic provenance that is different from their classification from the vibrational techniques. This opens a new realm of discussion about the possibility of ivory trade networks between the East and the West at the time of their production. To date, there has

been no evidence of Asian people crafting ivory in Portugal (Martin and Martin 2009), while the exportation of African ivory to Asian ivory workshops has been well-documented since the 10th century (Ferreira 2019c; Chaiklin 2010; Walker 2010). Additionally, this study provides a scientific perspective as to why African ivory was preferred in places as far as the East since ancient times, especially for carving intricate engraved pieces that would only be possible with soft ivory from East Africa. Since African elephants have marginally bigger tusks compared to Asian elephants, African ivory was also desired for carving larger pieces. Cultural factors also affect the demand for ivory, especially in Asian cultures. In South Asia, where the elephant-headed god Ganesha is worshipped, it is not usual to kill elephants for meat and tusks despite the high demand for ivory. Reverence for all living beings, including elephants, is also central to the religion of Hinduism, as well as Buddhism and Jainism (Chaiklin 2010). However, it is simplistic to assume that Asian cultures simply respect the elephant and thus ivory demand is suppressed. Perhaps a more nuanced perspective is that there is a huge disconnect between the high cultural regard given to elephants in South and Southeast Asia and the wholesale destruction of herds in Syria and North Africa (Walker 2010). Thus, there is also a gap between the artistic typologies associated with the community who produced it and the actual elephant origin that can otherwise only be bridged by an integrated set of approaches.

Table 10. Summary of classifications with FT-IR, FORS in the NIR, Raman, and Artistic Provenance. See Methodology for actual scale of pictures.

Sample	FT-IR	FORS-NIR	Raman*	Artistic Provenance
	-	AFRICAN	-	AFRICAN 21st CENTURY AD

AV1				
AV2	-	AFRICAN	-	AFRICAN 21st CENTURY AD
ES1	-	AFRICAN	-	AFRICAN 21st CENTURY AD
ES2	-	AFRICAN	-	AFRICAN 21st CENTURY AD
ES3	-	AFRICAN	-	AFRICAN 21st CENTURY AD
ES4	-	AFRICAN	-	AFRICAN 21st CENTURY AD
ES5	-	AFRICAN	-	AFRICAN 21st CENTURY AD

ES6	-	AFRICAN	-	AFRICAN 21st CENTURY AD
ES7	-	AFRICAN	-	AFRICAN 21st CENTURY AD
ES8	-	AFRICAN	-	AFRICAN 21st CENTURY AD
ES9	-	AFRICAN	-	AFRICAN 21st CENTURY AD
ES10	-	AFRICAN	-	AFRICAN 21st CENTURY AD
ES11	-	AFRICAN	-	AFRICAN 21st CENTURY AD

 FA1	-	AFRICAN	-	AFRICAN 21st CENTURY AD
 FA2	-	AFRICAN	-	AFRICAN 21st CENTURY AD
 FA3	-	AFRICAN	-	AFRICAN 21st CENTURY AD
 FG1	-	AFRICAN	-	AFRICAN 21st CENTURY AD
 FG2	-	AFRICAN	-	AFRICAN 21st CENTURY AD
 FG3	-	AFRICAN	-	AFRICAN 21st CENTURY AD
 PR1	-	AFRICAN	-	AFRICAN 21st CENTURY AD
 PR2	-	AFRICAN	-	AFRICAN 21st CENTURY AD

PR3	-	AFRICAN	-	AFRICAN 21st CENTURY AD
PR4	-	AFRICAN	-	AFRICAN 21st CENTURY AD
PU1	-	AFRICAN	-	AFRICAN 21st CENTURY AD
PU2	-	AFRICAN	-	AFRICAN 21st CENTURY AD
PU3	-	AFRICAN	-	AFRICAN 21st CENTURY AD
PU4	-	AFRICAN	-	AFRICAN 21st CENTURY AD
AV_ES1	-	AFRICAN	AFRICAN	ASIAN 20TH CENTURY AD

 AV_ES2	AFRICAN	AFRICAN	ASIAN	INDO-PORTUGUESE GOA LATE 17TH CENTURY AD
 AV_FG1	AFRICAN	AFRICAN	AFRICAN	ASIAN 20TH CENTURY AD
 CH_ES1	ASIAN	AFRICAN	-	CHINA 17TH CENTURY AD
 CH_ES2	AFRICAN	AFRICAN	-	CHINA 17TH CENTURY AD
 BJ1	-	AFRICAN	-	INDO-PORTUGUESE GOA
 BJ2	-	AFRICAN	-	INDO-PORTUGUESE GOA

BJ3	-	AFRICAN	-	INDO-PORTUGUESE GOA
BJ4	-	AFRICAN	-	INDO-PORTUGUESE GOA
IP_ES1	-	AFRICAN	-	INDO-PORTUGUESE
IP_ES2	-	AFRICAN	-	INDO-PORTUGUESE
SR_ES1	AFRICAN	AFRICAN	-	SRI LANKA (CEYLON) 17TH CENTURY AD
SR_ES2	ASIAN	AFRICAN	-	SRI LANKA (CEYLON) 17TH CENTURY AD

TL_ES1	-	AFRICAN	-	THAILAND 16TH TO 17TH CENTURY AD
TL_ES2	-	AFRICAN	-	THAILAND 17TH CENTURY AD
IV_SR1	-	AFRICAN	-	INDO-PORTUGUESE (?) WESTERN AFRICA, SIERRA LEONE 16TH TO 17TH CENTURY AD
IV_SR2	-	AFRICAN	-	INDO-PORTUGUESE WESTERN AFRICA, SIERRA LEONE 16TH TO 17TH CENTURY AD
PH_ES1	-	AFRICAN	-	MANILA, PHILIPPINES 17TH CENTURY AD
	ASIAN	ASIAN	-	CHINA 18TH TO 19TH CENTURY AD

1042				
1043	ASIAN	AFRICAN	-	CHINA 18TH TO 19TH CENTURY AD
841	-	AFRICAN	-	CHINA 18TH TO 19TH CENTURY AD
842	-	AFRICAN	-	
JC	-	AFRICAN	-	INDO-PORTUGUESE
17	-	AFRICAN	-	PORTUGUESE 16TH TO 17TH CENTURY AD
1054	-	AFRICAN	-	CHINA (?) OR INDIA (?) 17TH TO 19TH CENTURY AD

1055	-	AFRICAN	-	CHINA (?) OR INDIA (?) 17TH TO 19TH CENTURY AD
1061	-	AFRICAN	-	INDIA 18TH TO 19TH CENTURY AD
INV619	-	ASIAN	-	INDO-PORTUGUESE 17TH CENTURY AD
15	-	AFRICAN	-	AFRO-PORTUGUESE 1475 AD TO 1525 AD
16	-	AFRICAN	-	AFRO-PORTUGUESE 1475 AD TO 1525 AD
	-	AFRICAN	-	17TH CENTURY AD

19				
ESC817	-	AFRICAN	-	INDO-PORTUGUESE 17TH CENTURY AD
167ESC	-	AFRICAN	-	18TH CENTURY AD
2406	-	ASIAN	-	INDO-PORTUGUESE 17TH CENTURY AD
2492	-	ASIAN	-	INDO-PORTUGUESE 17TH CENTURY AD
2493	-	AFRICAN	-	INDO-PORTUGUESE 17TH CENTURY AD

2494	-	AFRICAN	-	INDO-PORTUGUESE 17TH CENTURY AD
2500	-	AFRICAN	-	INDO-PORTUGUESE 18TH CENTURY AD
2502	-	AFRICAN	-	INDO-PORTUGUESE 17TH CENTURY AD
2511	-	AFRICAN	-	INDO-PORTUGUESE 17TH CENTURY AD
JZ_TK	-	AFRICAN	AFRICAN	-
Elefante A	-	-	ASIAN	-
Elefante B	-	-	ASIAN	-

 Elefante C	-	-	ASIAN	-	P a g e
 BJ5	-	ANOMALOUS	-	-	
 2488	-	ANOMALOUS	-	-	
 2498	-	ANOMALOUS	-	-	
 2529	-	ANOMALOUS	-	-	

Conclusions

Are FT-IR, FORS-NIR, and Chemometrics Up to the Tusk?

Both spectroscopic techniques of FT-IR and FORS in the NIR combined with chemometric methods of PCA and PLS-DA were able to discriminate between Asian and African ivory objects. While FT-IR is comprehensive, it is also more time-consuming and limited to flat and polished sections of tusks and ivory objects. Thus, there were samples that were classified as inconclusive. The classification process was better with FORS in the NIR region since there were calibration samples of both Asian and African tusks. The entirety of samples was classified with a calibrated and cross-validated model, resulting in a TPR or sensitivity ranging from 93.028% to 99.020% in African samples while 93.333% to 100.000% in Asian samples.

This study demonstrated the potential of FORS-NIR as an efficient and robust technique for on-field ivory inspections. The development of a PLS-DA model to readily identify provenance of ivory objects and tusks saves time and costs by bringing the analysis on-field, making it an invaluable tool to resolve a long-standing multifaceted ecological and historic problem through archaeometry and chemometrics.

This investigation opens an interesting realm of discussion on the possible ivory trade networks during the production date of these historic ivory objects. Initially it might have been strange that ivory objects carved in Asia were revealed to be produced with African ivory, but due to African ivory's more desirable

mechanical properties, it might also have been requested more especially for large and more intricately carved pieces.

Recommendations

For future studies, variation of physical and chemical composition across sections should be considered by performing independent analyses on longitudinal and transverse sections. Since majority of the sample set used in this study were ivory objects, it was difficult to ascertain which part of the tusk was for analysis. Moreover, classification down to the subspecies level would also be valuable for specifying which region was the tusk sourced from. Since ivory objects that have lacquer or coatings cannot be characterized properly, techniques that are able to analyze beyond surface coatings are to be considered, such as Spatially offset Raman spectroscopy (SORS). Moreover, nondestructive micro-mechanical tests are of interest to characterize the mechanical properties of both African and Asian ivory.

References

Action for Elephants UK. 2018. "Blood Ivory, White Gold Funds Terrorism and Criminal Networks." 2018. https://actionforelephantsuk.org/information/blood-ivory/.

Albéric, M., A. Gourrier, W. Wagermaier, P. Fratzl, and I. Reiche. 2018. "The Three-Dimensional Arrangement of the Mineralized Collagen Fibers in Elephant Ivory and Its Relation to Mechanical and Optical Properties." *Acta Biomaterialia* 72 (May): 342–51. https://doi.org/10.1016/j.actbio.2018.02.016.

Amaral, Leonor. 2022. "Os Marfins Luso-Africanos Do Reino Do Benim (Séculos XVI-XVII). Estudo Histórico-Artístico e Material." Thesis Manuscript. Universidade de Lisboa.

Baker, Barry, Rachel Jacobs, Mary-Jacque Mann, Edgard Espinoza, and Giavanna Grein. 2020. *Identification Guide for Ivory and Ivory Substitutes*. Edited by Crawford Allan. 4th ed. Geneva, Switzerland: World Wildlife Fund (WWF) Washington DC. Commissioned by CITES Secretariat.

Beachey, R. W. 1967. "The East African Ivory Trade in the Nineteenth Century." *The Journal of African History* 8 (2): 269–90.

Betts, Alison, John Dodson, Ulf Garbe, Fiona Bertuch, and Gordon Thorogood. 2016. "A Carved Ivory Cylinder from Akchakhan-Kala, Uzbekistan: Problems of Dating and Provenance." *Journal of Archaeological Science: Reports* 5 (February): 190–96. https://doi.org/10.1016/j.jasrep.2015.10.034.

Blasco-Martín, Marta, Gianni Gallello, Lucía Soria-Combadiera, Eva Collado-Mataix, Agustín Pastor, and Consuelo Mata-Parreño. 2019. "Decoration Composition of Iberian Iron Age Ivory Artifacts Identified by No-Destructive Chemical Analyses." *Archaeological and Anthropological Sciences* 11 (7): 3561–76. https://doi.org/10.1007/s12520-018-00775-3.

Bortolaso, G, and J Roth, eds. 2008. "Elfenbein und Artenschutz (Ivory and Species Conservation); Proceedings of INCENTIVS - Meetings (204-2007)." Bundesamt für Naturschutz (BfN). https://citeseerx.ist.psu.edu/viewdoc/download?doi=10.1.1.686.263&rep=rep1&type=pdf.

Brody, Rachel H, Howell G. M Edwards, and A. Mark Pollard. 2001. "Chemometric Methods Applied to the Differentiation of Fourier-Transform Raman Spectra of Ivories." *Analytica Chimica Acta* 427 (2): 223–32. https://doi.org/10.1016/S0003-2670(00)01206-X.

Burragato, F, S Materazzi, R Curini, and G Ricci. 1998. "New Forensic Tool for the Identification of Elephant or Mammoth Ivory." *Forensic Science International* 96 (2–3): 189–96. https://doi.org/10.1016/S0379-0738(98)00128-5.

Cartier, Laurent E., Michael S. Krzemnicki, Mario Gysi, Bertalan Lendvay, and Nadja V. Morf. 2020. "A Case Study of Ivory Species Identification Using a Combination of Morphological, Gemmological and Genetic Methods." *The Journal of Gemmology* 37 (3): 282–97. https://doi.org/10.15506/JoG.2020.37.3.282.

Céline, Chadefaux, Anne-Solenn Le Hô, Ludovic Bellot-Gurlet, and Ina Reiche. 2009. "Curve-Fitting Micro-ATR-FTIR Studies of the Amide I and II Bands of Type I Collagen in Archaeological Bone Materials." *E-Preservation Science* 6 (January): 129–37.

Chaiklin, Martha. 2010. "Ivory in World History – Early Modern Trade in Context." *History Compass* 8 (6): 530–42. https://doi.org/10.1111/j.1478-0542.2010.00680.x.

Chaitae, Apinya, Iain J. Gordon, Jane Addison, and Helene Marsh. 2022. "Protection of Elephants and Sustainable Use of Ivory in Thailand." *Oryx* 56 (4): 601–8. https://doi.org/10.1017/S0030605321000077.

Chaitae, Apinya, Ronnarit Rittiron, Iain J. Gordon, Helene Marsh, Jane Addison, Suttahatai Pochanagone, and Nattakan Suttanon. 2021. "Shining NIR Light on

Ivory: A Practical Enforcement Tool for Elephant Ivory Identification." *Conservation Science and Practice* 3 (9). https://doi.org/10.1111/csp2.486.

Choudhury, Anwaruddin. 1999. "Status and Conservation of the Asian Elephant Elephas Maximus in North-Eastern India." *Mammal Review* 29 (3): 141–74. https://doi.org/10.1046/j.1365-2907.1999.00045.x.

CITES. 2020. "Monitoring the Illegal Killing of Elephants (MIKE). Report: PIKE Trend Analysis -- Methodology and Results." https://cites.org/eng/MIKE_PIKE_Trends_report_elephants_CITES_16112020.

Clauss, Marcus, and Donald E. Paglia. 2012. "Iron Storage Disorders in Captive Wild Mammals: The Comparative Evidence." *Journal of Zoo and Wildlife Medicine: Official Publication of the American Association of Zoo Veterinarians* 43 (3 Suppl): S6-18. https://doi.org/10.1638/2011-0152.1.

Conard, Nicholas J. 2009. "A Female Figurine from the Basal Aurignacian of Hohle Fels Cave in Southwestern Germany." *Nature* 459 (7244): 248–52. https://doi.org/10.1038/nature07995.

Coutu, Ashley N., Julia Lee-Thorp, Matthew J. Collins, and Paul J. Lane. 2016. "Mapping the Elephants of the 19th Century East African Ivory Trade with a Multi-Isotope Approach." Edited by Faysal Bibi. *PLOS ONE* 11 (10): e0163606. https://doi.org/10.1371/journal.pone.0163606.

Coutu, Ashley N., Gavin Whitelaw, Petrus le Roux, and Judith Sealy. 2016. "Earliest Evidence for the Ivory Trade in Southern Africa: Isotopic and ZooMS Analysis of Seventh–Tenth Century Ad Ivory from KwaZulu-Natal." *African Archaeological Review* 33 (4): 411–35. https://doi.org/10.1007/s10437-016-9232-0.

Cowger, Win, Zacharias Steinmetz, Andrew Gray, Keenan Munno, Jennifer Lynch, Hannah Hapich, Sebastian Primpke, Hannah De Frond, Chelsea Rochman, and Orestis Herodotou. 2021. "Microplastic Spectral Classification Needs an Open Source Community: Open Specy to the Rescue!" *Analytical Chemistry* 93 (21): 7543–48. https://doi.org/10.1021/acs.analchem.1c00123.

Duffy, Rosaleen. 2022. "Crime, Security, and Illegal Wildlife Trade: Political Ecologies of International Conservation." *Global Environmental Politics* 22 (2): 23–44. https://doi.org/10.1162/glep_a_00645.

Edwards, H. G. M, and D. W Farwell. 1995. "Ivory and Simulated Ivory Artefacts: Fourier Transform Raman Diagnostic Study." *Spectrochimica Acta Part A: Molecular and Biomolecular Spectroscopy* 51 (12): 2073–81. https://doi.org/10.1016/0584-8539(95)01455-3.

Edwards, H. G. M., D. W. Farwell, J. M. Holder, and E. E. Lawson. 1997a. "Fourier-Transform Raman Spectra of Ivory III: Identification of Mammalian Specimens." *Spectrochimica Acta Part A: Molecular and Biomolecular Spectroscopy*, Applications of Fourier Transform Raman Spectroscopy - VII, 53 (13): 2403–9. https://doi.org/10.1016/S1386-1425(97)00180-7.

———. 1997b. "Fourier-Transform Raman Spectroscopy of Ivory: II. Spectroscopic Analysis and Assignments." *Journal of Molecular Structure* 435 (1): 49–58. https://doi.org/10.1016/S0022-2860(97)00122-1.

Edwards, H. G. M., N. F. Nik Hassan, and N. Arya. 2006. "Evaluation of Raman Spectroscopy and Application of Chemometric Methods for the Differentiation of Contemporary Ivory Specimens I: Elephant and Mammalian Species." *Journal of Raman Spectroscopy* 37 (1–3): 353–60. https://doi.org/10.1002/jrs.1458.

Edwards, Howell. 1998. "Fourier Transform-Raman Spectroscopy of Ivory: A Non-Destructive Diagnostic Technique," 9.

Edwards, Howell G. M., Susana E. Jorge Villar, Nik F. Nik Hassan, Nlin Arya, Sonia O'Connor, and Donna M. Charlton. 2005. "Ancient Biodeterioration: An FT–Raman Spectroscopic Study of Mammoth and Elephant Ivory." *Analytical and Bioanalytical Chemistry* 383 (4): 713–20. https://doi.org/10.1007/s00216-005-0011-z.

Espinoza, Edgard, and Mary-Jacque Mann. 1999. "Identification Guide for Ivory and Ivory Substitutes." World Wildlife Fund (WWF) and the Conservation Foundation. https://cites.org/sites/default/files/eng/resources/pub/E-Ivory-guide.pdf.

Fagg, W. P., and William Buller Fagg. 1959. *Afro-Portuguese Ivories*. Batchworth Press.

Ferreira, Jorge. 2019a. "Indo-Portuguese Ivories." In *From Lisbon to Japan: The Portuguese Empire in the 16th and 17th Centuries*, 54–55. Lisbon, Portugal: São Roque | Antiguidades & Galeria de Arte.

———. 2019b. "Kingdom of Siam, Thailand." In *From Lisbon to Japan: The Portuguese Empire in the 16th and 17th Centuries*, 152–53. Lisbon, Portugal: São Roque | Antiguidades & Galeria de Arte.

———. 2019c. "Sinhalese-Portuguese Ivories." In *From Lisbon to Japan: The Portuguese Empire in the 16th and 17th Centuries*, 132–33. Lisbon, Portugal: São Roque | Antiguidades & Galeria de Arte.

Godfrey, I. M., E. L. Ghisalberti, E. W. Beng, L. T. Byrne, and G. W. Richardson. 2002. "The Analysis of Ivory from a Marine Environment." *Studies in Conservation* 47 (1): 29–45. https://doi.org/10.2307/1506833.

Guennec, Yannick Le. 2020. "African Elephant Ivory Subspecies Differentiation by Raman, FTIR and UV-Vis Spectroscopic Analysis," 21.

Guérin, Sarah M. 2010. "Ivory Carving in the Gothic Era, Thirteenth–Fifteenth Centuries." In *Heilbrunn Timeline of Art History*. New York: The Metropolitan Museum of Art, 2000-. https://www.metmuseum.org/toah/hd/goiv/hd_goiv.htm.

Hargreaves, Michael, Neil Macleod, Victoria Brewster, Tasnim Munshi, H. Edwards, and Pavel Matousek. 2009. "Application of Portable Raman Spectroscopy and Benchtop Spatially Offset Raman Spectroscopy to Interrogate Concealed Biomaterials." *Journal of Raman Spectroscopy* 40 (December): 1875–80. https://doi.org/10.1002/jrs.2335.

Hauenstein, Severin, Mrigesh Kshatriya, Julian Blanc, Carsten F. Dormann, and Colin M. Beale. 2019. "African Elephant Poaching Rates Correlate with Local Poverty, National Corruption and Global Ivory Price." *Nature Communications* 10 (1): 2242. https://doi.org/10.1038/s41467-019-09993-2.

Hill, Shannen. 2018. "The Art of African Ivory." Agnes Publications. https://agnes.queensu.ca/site/uploads/2018/05/AEAC_AfricanIvory_forweb_2May2018.pdf.

Horta, José da Silva, Carlos Almeida, and Peter Mark. 2021. *African Ivories in the Atlantic World, 1400-1900*. Centro de História da Universidade de Lisboa.

"How Japan Is Fueling the Slaughter of Elephants." 2015. Animals. December 10, 2015. https://www.nationalgeographic.com/animals/article/151210-Japan-ivory-trade-african-elephants.

Hsiang, Solomon, and Nitin Sekar. 2016. "Does Legalization Reduce Black Market Activity? Evidence from a Global Ivory Experiment and Elephant Poaching Data." Working Paper 22314. Working Paper Series. National Bureau of Economic Research. https://doi.org/10.3386/w22314.

Humane Society International. 2014. "Elephant-Related Trade Timeline." Humane Society International. https://www.hsi.org/wp-content/uploads/assets/pdfs/Elephant_Related_Trade_Timeline.pdf.

IUCN. 2018. "The Status of Asian Elephants." World Wildlife Fund. 2018. https://www.worldwildlife.org/magazine/issues/winter-2018/articles/the-status-of-asian-elephants.

———. 2021. "African Elephant Species Now Endangered and Critically Endangered - IUCN Red List." IUCN. March 25, 2021. https://www.iucn.org/news/species/202103/african-elephant-species-now-endangered-and-critically-endangered-iucn-red-list.

Jirik, Kate. 2021. "LibGuides: Asian Elephant (Elephas Maximus) Fact Sheet: Population & Conservation Status." 2021. https://ielc.libguides.com/sdzg/factsheets/asianelephant/population.

Koirala, Raj Kumar, David Raubenheimer, Achyut Aryal, Mitra Lal Pathak, and Weihong Ji. 2016. "Feeding Preferences of the Asian Elephant (Elephas Maximus) in Nepal." *BMC Ecology* 16 (1): 54. https://doi.org/10.1186/s12898-016-0105-9.

Kolmas, Joanna, Dariusz Marek, and Waclaw Kolodziejski. 2015. "Near-Infrared (NIR) Spectroscopy of Synthetic Hydroxyapatites and Human Dental Tissues." *Applied Spectroscopy* 69 (8): 902–12.

LeGeros, R. Z., O. R. Trautz, E. Klein, and J. P. LeGeros. 1969. "Two Types of Carbonate Substitution in the Apatite Structure." *Experientia* 25 (1): 5–7. https://doi.org/10.1007/BF01903856.

Long, D. A., H. G. M. Edwards, and D. W. Farwell. 2008. "The Goodmanham Plane: Raman Spectroscopic Analysis of a Roman Ivory Artefact." *Journal of Raman Spectroscopy: An International Journal for Original Work in All Aspects of Raman Spectroscopy, Including Higher Order Processes, and Also Brillouin and Rayleigh Scattering* 39 (3): 322–30.

Madupalli, Honey, Barbara Pavan, and Mary M.J. Tecklenburg. 2017. "Carbonate Substitution in the Mineral Component of Bone: Discriminating the Structural Changes, Simultaneously Imposed by Carbonate in A and B Sites of Apatite." *Journal of Solid State Chemistry* 255 (November): 27–35. https://doi.org/10.1016/j.jssc.2017.07.025.

Martin, Esmond, and Chryssee Martin. 2009. "Portugal's Long Association with African Ivory." *Pachyderm* 46 (December): 35–46.

McConnell, Duncan. 1965. "Crystal Chemistry of Hydroxyapatite: Its Relation to Bone Mineral." *Archives of Oral Biology* 10 (3): 421–31. https://doi.org/10.1016/0003-9969(65)90107-X.

Meyer, Jordana M., Naftali Honig, and Elizabeth A. Hadly. 2022. "Diet DNA Reveals Novel African Forest Elephant Ecology on the Grasslands of the Congo Basin." *Environmental DNA* 4 (4): 846–67. https://doi.org/10.1002/edn3.296.

Mujica, Luis, José Rodellar, Alfredo Guemes, and J. López-Diez. 2008. "PCA Based Measures: Q-Statistic and T2-Statistic for Assessing Damages in Structures." *Proceedings of the 4th European Workshop on Structural Health Monitoring*, January, 1088–95.

Nocete, F., J.M. Vargas, T.X. Schuhmacher, A. Banerjee, and W. Dindorf. 2013. "The Ivory Workshop of Valencina de La Concepción (Seville, Spain) and the Identification of Ivory from Asian Elephant on the Iberian Peninsula in the First Half of the 3rd Millennium BC." *Journal of Archaeological Science* 40 (3): 1579–92. https://doi.org/10.1016/j.jas.2012.10.028.

O'Connor, Sonia, Howell G. M. Edwards, and Esam Ali. 2011. "An Interim Investigation of the Potential of Vibrational Spectroscopy for the Dating of Cultural Objects in Ivory." *ArcheoSciences. Revue d'archéométrie*, no. 35 (April): 159–65. https://doi.org/10.4000/archeosciences.3091.

O'Connor, T.P. 1984. "On the Structure, Chemistry and Decay of Bone, Antler and Ivory." University of York. https://canvas.gu.se/courses/54791/files/5708781/download?download_frd=1.

Parungao, Dorothy, Peter Vandenabeele, Howell G.M. Edwards, Antonio Candeias, and Catarina Miguel. "Mobile Raman Spectroscopy Analysis of Elephant Ivory Objects." Journal of Raman Spectroscopy, 2022. https://doi.org/10.1002/jrs.6487.

Payne, K. J., and A. Veis. 1988. "Fourier Transform Ir Spectroscopy of Collagen and Gelatin Solutions: Deconvolution of the Amide I Band for Conformational Studies." *Biopolymers* 27 (11): 1749–60. https://doi.org/10.1002/bip.360271105.

"Poaching behind Worst African Elephant Losses in 25 Years – IUCN Report." 2016. IUCN. September 23, 2016. https://www.iucn.org/news/species/201609/poaching-behind-worst-african-elephant-losses-25-years-%E2%80%93-iucn-report.

Power, A. C., J. Chapman, S. Chandra, J. J. Roberts, and D. Cozzolino. 2018. "Illuminating the Flesh of Bone Identification – An Application of near Infrared Spectroscopy." *Vibrational Spectroscopy* 98 (September): 64–68. https://doi.org/10.1016/j.vibspec.2018.07.011.

Power, Aoife, Sandy Ingleby, James Chapman, and Daniel Cozzolino. 2019. "Lighting the Ivory Track: Are Near-Infrared and Chemometrics Up to the Job? A Proof of Concept." *Applied Spectroscopy* 73 (7): 816–22. https://doi.org/10.1177/0003702819837297.

Raubenheimer, E.J, J.M.M Brown, D.B.K Rama, M.J Dreyer, P.D Smith, and J Dauth. 1998. "Geographic Variations in the Composition of Ivory of the African Elephant (Loxodonta Africana)." *Archives of Oral Biology* 43 (8): 641–47. https://doi.org/10.1016/S0003-9969(98)00051-X.

Rijkelijkhuizen, M. J., L. M. Kootker, and G. R. Davies. 2015. "Multi-Isotope Analysis of Elephant Ivory Artefacts from Amsterdam: A Preliminary Provenance Study." *World Archaeology* 47 (3): 504–24. https://doi.org/10.1080/00438243.2015.1024884.

Rosen, Rebecca J. 2012. "What Is It About an Elephant's Tusks That Make Them So Valuable?" The Atlantic. September 6, 2012. https://www.theatlantic.com/business/archive/2012/09/what-is-it-about-an-elephants-tusks-that-make-them-so-valuable/262021/.

Rozalen, M., and A. Ruiz Gutierrez. 2015. "A Study of the Origin and Gilding Technique of a Hispano-Philippine Ivory from the XVIIth Century." *Journal of Archaeological Science: Reports* 4 (December): 1–7. https://doi.org/10.1016/j.jasrep.2015.08.034.

Ryder, Alan FC. 1964. "A Note on the Afro-Portuguese Ivories." *The Journal of African History* 5 (3): 363–65.

Schmidberger, Andreas, Bernhard Durner, David Gehrmeyer, and Robert Schupfner. 2018. "Development and Application of a Method for Ivory Dating by Analyzing Radioisotopes to Distinguish Legal from Illegal Ivory." *Forensic Science International* 289 (August): 363–67. https://doi.org/10.1016/j.forsciint.2018.06.016.

Singh, Rina Rani, Surendra Prakash Goyal, Param Pal Khanna, Pulok Kumar Mukherjee, and Raman Sukumar. 2006. "Using Morphometric and Analytical Techniques to Characterize Elephant Ivory." *Forensic Science International* 162 (1–3): 144–51. https://doi.org/10.1016/j.forsciint.2006.06.028.

Strauss, Mark. 2015. "Who Buys Ivory? You'd Be Surprised." *National Geographic*, August 12, 2015. https://www.nationalgeographic.com/pages/article/150812-elephant-ivory-demand-wildlife-trafficking-china-world.

Sun, Xueying, Mingyue He, and Jinlin Wu. 2022. "Crystallographic Characteristics of Inorganic Mineral in Mammoth Ivory and Ivory." *Minerals* 12 (2): 117. https://doi.org/10.3390/min12020117.

Terborgh, John, Lisa C. Davenport, Lisa Ong, and Ahimsa Campos-Arceiz. 2018. "Foraging Impacts of Asian Megafauna on Tropical Rain Forest Structure and Biodiversity." *Biotropica* 50 (1): 84–89. https://doi.org/10.1111/btp.12488.

Tikkanen, Amy. 2022. "Manueline | Architectural Style | Britannica." 2022. https://www.britannica.com/art/Manueline.

Trapani, Josh, and Daniel C. Fisher. 2003. "Discriminating Proboscidean Taxa Using Features of the Schreger Pattern in Tusk Dentin." *Journal of Archaeological Science* 30 (4): 429–38. https://doi.org/10.1006/jasc.2002.0852.

Tripati, Sila, and Ian Godfrey. 2007. "Studies on Elephant Tusks and Hippopotamus Teeth Collected from the Early 17th Century Portuguese Shipwreck off Goa,

West Coast of India: Evidence of Maritime Trade between Goa, Portugal and African Countries." *CURRENT SCIENCE* 92 (3): 8.

Valera, António Carlos, Thomas Xaver Schuhmacher, and Arun Banerjee. 2015. "Ivory in the Chalcolithic Enclosure of Perdigões (South Portugal): The Social Role of an Exotic Raw Material." *World Archaeology* 47 (3): 390–413. https://doi.org/10.1080/00438243.2015.1014571.

Virág, Attila. 2012. "Histogenesis of the Unique Morphology of Proboscidean Ivory." *Journal of Morphology* 273 (12): 1406–23. https://doi.org/10.1002/jmor.20069.

Walker, John Frederick. 2010. *Ivory's Ghosts: The White Gold of History and the Fate of Elephants*. Open Road+ Grove/Atlantic.

Wang, Kai, Yuhang He, Ruiqi Shao, Hao Zhao, Honglin Ran, Yu Lei, and Yihang Zhou. 2022. "FTIR Study on the Phase Transition of Experimental and Archaeological Burnt Ivory." *Heritage Science* 10 (1): 131. https://doi.org/10.1186/s40494-022-00769-4.

Wehrmeister, U, T M Gluhak, H Götz, and D E Jacob. 2013. "Differentiation of African and Asian Elephant Dentine by FT- Raman Spectros- Copy and Chemometric Methods." In , 6. Hanoi, Vietnam.

Wildlife Justice Commission. 2020. "The Rapid Growth in the Industrial Scale Trafficking of Pangolin Scales." February 2020. https://wildlifejustice.org/new-report-analyses-unprecedented-levels-of-pangolin-trafficking-urging-stakeholders-to-tackle-it-as-transnational-crime/.

Wingender, Brian, Masashi Azuma, Christina Krywka, Paul Zaslansky, John Boyle, and Alix Deymier. 2021. "Carbonate Substitution Significantly Affects the Structure and Mechanics of Carbonated Apatites." *Acta Biomaterialia* 122 (March): 377–86. https://doi.org/10.1016/j.actbio.2021.01.002.

Workman, Jerry, and Lois Weyer. 2008. *Practical Guide and Spectral Atlas for Interpretive Near-Infrared Spectroscopy*. 1st ed. CRC Press. https://www.routledge.com/Practical-Guide-and-Spectral-Atlas-for-Interpretive-Near-Infrared-Spectroscopy/Workman-Jr-Weyer/p/book/9781439875254.

World Wildlife Fund. 2022. "Asian Elephant." World Wildlife Fund. 2022. https://www.worldwildlife.org/species/asian-elephant.

Yin, Zuowei, Pengfei Zhang, Quanli Chen, Qinfeng Luo, Chen Zheng, and Yuling Li. 2013. "A Comparison of Modern and Fossil Ivories Using Multiple Techniques." *Gems & Gemology* 49 (1): 16–27. https://doi.org/10.5741/GEMS.49.1.16.

Appendix

I. Instrument Specifications

Fourier-Transform Infrared (FT-IR) Spectrometer

The analysis was performed using the FT-IR spectrometer ALPHA from Bruker. It is fitted with wear-free components such as the RockSolid interferometer and a durable solid-state diode laser. Due to its small size, the ALPHA can be used in a wide range of applications for educational and research applications. Aside from food and beverages, pharmaceuticals, and forensic drug analysis, the spectrometer was used in this research for analysis of precious ivory artifacts.

The ALPHA spectrometer is accompanied with the OPUS 7.0 software for data acquisition and transformation. The mode of acquisition can be in transmission, attenuated total reflectance (ATR), and diffuse and specular reflection modes – based on the component that is fitted into the ALPHA spectrometer.

UV-VIS NIR Fiber Optics Reflectance Spectrometer (UV-Vis-NIR FORS)

The characterization was performed using a full-range broadband mobile spectrometer (i-Spec® 25) with a handheld reflectance probe for measurements across the Vis-NIR range from 400-2500 nm, both developed by B&W Tek. The spectrometer is an air-cooled system with Si, InGaAs, and extended InGaAs array sensors for the detectors.

The spectrometer is equipped with a handheld reflectance probe with integrated 5W tungsten halogen source (model: TRP5). It is a TFA bundle – trifurcated fiber optic

bundle. This means it combines optical fibers at a common end with the fiber optic bundle separating into three separate channels.

The white reference material is a PTFE (polytetrafluoroethylene) - Halon G-50 transfer reference that has a diameter of 1.25 in. It is in the model SRR-1.25-99 from B&W-TEK with the following reflectance values in the three EM regions:

Region	Reflectance
400 nm - 800 nm	>99%
300 nm - 1800 nm	>98%
250 nm - 2500 nm	>92%

II. MATLAB codes

Getting the FORS-Vis-NIR data

```
fileDir = cd;
a=dir('*.csv');
clear Data Filenames Class
for k=1:length(a)
disp(['Importing ' a(k).name]);
Filenames{k,1}=a(k).name;
d = textread(a(k).name,'','headerlines',1,'delimiter',',');
if k==1;WL=d(:,1)';end
Data(k,:)=d(:,7)';
if isequal(upper(a(k).name(1:2)),'IV')
Class{k,1}='African';
else
Class{k,1}='Asian';
end
end
clear d k a;
```

Getting the FT-IR data

```
fileDir = cd;
a=dir('*.csv');
clear Data Filenames Class
for k=1:length(a)
disp(['Importing ' a(k).name]);
Filenames{k,1}=a(k).name;
d = textread(a(k).name,'','delimiter','\t');
if k==1;WL=d(:,1)';end
Data(k,:)=d(:,2)';
if isequal(upper(a(k).name(1:2)),'IV')
Class{k,1}='African';
else
Class{k,1}='Asian';
end
end
clear d k a;
```

III. Information for the Ivory Pieces

The ivory samples used in this study were procured from environmental organizations, museums, and private collections.

Jardim Zoológico (Lisbon)

TSK Date: 21st century Origin: African elephant, female, young.	
Fallen incisor from one of the young African-origin elephants in Jardim Zoológico in Lisbon.	

Royal Elephant Kraal Village (Bangkok)

Elefante A Date: 21st century Origin: Asian elephant	
Fallen tusk from one of the elephants in Royal Elephant Kraal Village in Bangkok, Thailand.	

Elefante B Date: 21st century Origin: Asian elephant	
Fallen tusk from one of the elephants in Royal Elephant Kraal Village in Bangkok, Thailand.	

Elefante C Date: 21st century Origin: Asian elephant	
Fallen tusk from one of the elephants in Royal Elephant Kraal Village in Bangkok, Thailand.	

Instituto da Conservação da Natureza e das Florestas

AV1 Date: 21st century Origin: Airport customs for African-bound and -return flights	
Worked tusk with a hollow inside, carved in the shape of a bird.	

AV2 Date: 21st century Origin: Airport customs for African-bound and -return flights	
Worked tusk with a hollow inside, carved in the shape of a bird.	

ES1 Date: 21st century Origin: Airport customs for African-bound and -return flights	
Worked tusk in the shape of a woman with markedly African features, carrying a vase upon her head.	

ES2 Date: 21st century Origin: Airport customs for African-bound and -return flights	
Worked tusk in the shape of a woman with markedly African features, tagging along a small child.	

ES3 Date: 21st century Origin: Airport customs for African-bound and -return flights	
Carved ivory resembling a woman with markedly African features, hair tied back with front braids, and wearing a blouse and a necklace. The figure is tilted towards their right.	

ES4 Date: 21st century Origin: Airport customs for African-bound and -return flights	
Worked tusk in the shape of a woman with braids, with the headpiece signifying it as a high-status figure.	

ES5 Date: 21st century Origin: Airport customs for African-bound and -return flights	
Worked tusk in the shape of a woman with braids, with the headpiece signifying it as a high-status figure.	

ES6 Date: 21st century Origin: Airport customs for African-bound and -return flights	
Carved ivory in the figure of a woman tilted to her right. The figure has braids, wearing a blouse, and has markedly African features.	

ES7	
Date: 21st century	
Origin: Airport customs for African-bound and -return flights	

Elongated carved ivory in the shape of an antelope's head, with a recurring geometric pattern that culminates in a layered base.

ES8	
Date: 21st century	
Origin: Airport customs for African-bound and -return flights	

Carved ivory in the figure of a woman tilted to her right. The figure has braids, wearing a blouse, and has markedly African features.

ES9	
Date: 21st century	
Origin: Airport customs for African-bound and -return flights	

Carved ivory in the shape of a nude male figure, from the stomach up, tilted towards their left.

ES10	
Date: 21st century Origin: Airport customs for African-bound and -return flights	
Carved ivory in the shape of a sitted male figure, facing front but towards the viewers' right.	

ES11	
Date: 21st century Origin: Airport customs for African-bound and -return flights	
Carved ivory figure of a male with an adorned headpiece, with mouth agape, possibly in the middle of performing a musical ritual, as evidenced by the instrument.	

FA1	
Date: 21st century Origin: Airport customs for African-bound and -return flights	
Polished ivory carved in the shape of a fruit.	

FA2	
Date: 21st century	

Origin: Airport customs for African-bound and -return flights	
Polished ivory carved in the shape of a fruit.	

FA3 Date: 21st century Origin: Airport customs for African-bound and -return flights	
Worked ivory in the shape of what appears to be an antelope, mounted on the same ivory base.	

FG1 Date: 21st century Origin: Airport customs for African-bound and -return flights	
Polished and straight-edged ivory knife adorned with a carved figure at the end.	

FG2 Date: 21st century Origin: Airport customs for African-bound and -return flights	
Polished ivory knife with wavy edges, and the handle carved in what appears to be a cactus.	

FG3	
Date: 21st century	
Origin: Airport customs for African-bound and -return flights	
Ivory fork with two prongs and a hole at the end for hanging.	

PR1	
Date: 21st century	
Origin: Airport customs for African-bound and -return flights	
Worked tusk with the base adorned with the frontal feature of a woman with African features, braided hair, and a necklace.	

PR2	
Date: 21st century	
Origin: Airport customs for African-bound and -return flights	
Worked tusk with the base adorned with the frontal feature of a figure with African features.	

PR3	
Date: 21st century Origin: Airport customs for African-bound and -return flights	
Worked tusk with the base adorned with the frontal feature of a figure with African features.	

PR4	
Date: 21st century Origin: Airport customs for African-bound and -return flights	

PU1	
Date: 21st century Origin: Airport customs for African-bound and -return flights	
Open and simple ivory bangle with smoothed edges and surfaces.	

PU2	
Date: 21st century Origin: Airport customs for African-bound and -return flights	

Open and simple ivory bangle with smoothed edges and surfaces.	

PU3 Date: 21st century Origin: Airport customs for African-bound and -return flights	
Open and simple ivory bangle with smoothed edges and surfaces.	

PU4 Date: 21st century Origin: Airport customs for African-bound and -return flights	
Closed and decorated ivory bangle with a carved, flowing surface.	

Museu Nacional de Arte Antiga

17 ESC Date: 16th to 17th century AD Production: Portuguese	
Standing and frontal, the two figures wear short tunics that, falling over their knees, reveal balloon pants. The long hair, tied at the nape of the neck, leaves the hair combed in a horse	

robo loose. Seated on a circular pedestal with a regular cut Dynamic sculptural set in the plastic treatment of the drapes and in the animation of the dialogue shown by the expression of the faces Sculpture of Pieno figure.

19 ESC

Date: 17th century (?) AD

Seated and frontal, the female figure supports his head with his right hand. With straight hair, he wears a smooth tunic, structured in parallel vertical breeches with a straight profile, allowing a glimpse of the shod feet Over the tunic, he wears a long cloak, thrown in the back and grouped over the right knee, structuring itself in oblique pleats with a curved profile falling down staggered at the height of the legs. Dynamic in the treatment of drapes. Full-length sculpture.

2495 ESC

Date: 17th century (?) AD

Production: Indo-Portuguese (?)

Baby Jesus in ivory, lying down, with his right hand resting on his chest.

2493 ESC

Date: 17th century AD

Production: Indo-Portuguese

Virgin in ivory with folded hands at waist level. Presents the hair up to the waist and wears a cloak over a tunic, both pleated.

2406 ESC

Date: 17th century AD

Production: Indo-Portuguese

Virgin represented standing, frontal, with the Child Jesus seated on her left arm, also frontal. crowned In her right hand she holds a rosary with round beads and a cross at the end. Wears a dress and cloak. The dress is crafted in vertical pleats with a round profile over the legs, draped in ruffles over the moon crescent. The cloak is thrown over the back.

The lunar crescent is highlighted on the base, which is round.

Static.

2511 ESC

Date: 17th century AD

Production: Indo-Portuguese

Ivory plaque, rectangular, carved, with representation of the Immaculate Conception and two cherubs in the upper corners. Background with balls of clouds.

2488 ESC	
Date: 17th century AD	
Production: Indo-Portuguese	
Oratory miniature with image of the Virgin in ivory inside a cylindrical-shaped temple, topped by a dome ending in a small pinnacle, and with an interior painted in red. The figure, with folded hands, wears a tunic.	

2529 ESC	
Date: 17th century (?) AD	
Production: Indo-Portuguese	
Baby Jesus in ivory, on a pedestal, wearing a tunic and mantle. He holds with his right hand a silver crucifix, and with his left a small base with an orifice, where the terrestrial globe would be placed.	

2492 ESC	
Date: 17th century (?) AD	
Production: Indo-Portuguese	
Female figure lying down, with her head propped on her right hand and a book resting on her other hand. He has hair up to his belt and wears a tunic under a cloak.	

619 ESC Date: 17th century AD Production: Indo-Portuguese	
The Baby Jesus, front. Sitting and cross-legged, he has his head turned to the right and resting on his hand. He wears a sheepskin bag and wears sandals. On the lap and on the shoulders, the lambs stare at the observer. It is based on the Monte Sacro, with a conical structure, which houses images of saints and symbolic animals wrapped in plant decoration. Static. Pieno figure sculpture.	

817 ESC Date: 17th century AD Production: Indo-Portuguese	
Ivory image, carved in two pieces (figure and pedestal), representing the Virgin standing, with hands in prayer position, based on lunar crescent. He wears tunic cinched at the waist and cloak over the shoulders, both with accentuated pleats and edges worked with a cutout motif and dotted circles. Bare hair, worked in wavy locks, softer in the back. Plinth decorated with three registers of stylized acanthus leaves, except in the back, where it is only smooth. Traces of polychromy in black.	

2498 ESC	
Date: 17th century AD	
Production: Indo-Portuguese	

Image in martin, carved in a single piece, representing the Virgin standing, based on a lunar crescent, with her hands in prayer position. He wears tunic cinched at the waist and cloak over the shoulders, both with accentuated pleats and edges worked with a slight cutout and pearl motif. Bare hair, worked in wavy locks, separated from each other. Application of gold in the hair and edges of the clothes and traces of polychromy in the eyes and lips.

2502 ESC	
Date: 17th century AD	
Production: Indo-Portuguese	

Ivory image, carved in a single piece, representing a female figure standing with her hands crossed over her chest, and her head turned up. She wears a tunic cinched at the waist, a cloak over her shoulders and a veil, all with accentuated pleats. Traces of polychrome on the edges of the garments.

2500 ESC Date: 18th century AD Production: Indo-Portuguese	
Ivory image, carved in a single piece, representing a female figure standing, with hands clasped in prayer position. He wears a tunic cinched at the waist and a mantle over his head and shoulders. Traces of red polychrome on the garments. The back of the figure is smooth.	

2499 ESC Date: 17th century AD Production: Indo-Portuguese	
Ivory image, carved in a single piece, representing the Virgin standing, based on a lunar crescent, with her hands in prayer position. He wears a tunic cinched at the waist and a mantle over his shoulders, both with accentuated pleats and edges worked with a slight cutout motif. Hair uncovered, down to the waist, with a slight wave. Traces of polychromy in the hair, tunic edges and neckline.	

2494 ESC	
Date: 17th century AD	
Production: Indo-Portuguese	

Figure of St. John the Evangelist, holding a closed book against his body with his left hand, and resting his right hand on his chest. With long hair over the shoulders, the figure wears a tunic with vertical pleats and, over this, a cloak that is thrown over the left shoulder, forming a flap at the front.

842 ESC	
Date: 17th century AD	
Production: Afro-Portuguese	

Figure of a woman, standing, frontal and naked. Hold a bottle in your left hand. Macrocephaly Oblong face, dilated eyeballs, full cheekbones, thick nose and lips. Static. Full-length sculpture

16 ESC Date: 1475 AD to 1525 AD Production: Afro-Portuguese	

Saint John the Evangelist, standing and frontal, takes his right hand to his chest and with his left hand holds the flap of the mantle and the Book of the Gospels, closed. grooved in ivory, with a curved profile and showing bare feet. Over the tunic, he wears a mantle thrown on the back, grouped under the right forearm with a flap thrown on the left, structured in round pleats to suggest movement, Dynamic in the plastic treatment of the drapes.

15 ESC Date: 1475 AD to 1525 AD Production: Afro-Portuguese	

The Virgin, standing and frontal, presents her head covered by a veil and her hands folded, in a prayerful attitude. Face with an oblong structure: high forehead, almond-shaped eyes, straight nose, thin lips. He wears a smooth tunic, structured in vertical pleats with a round profile that, falling superimposed, hides the feet. Over the tunic he wears a cloak thrown over his head and shoulders. Tucked under the forearms, the mantle is structured in strong curved pleats Dynamic, suggesting movement with the slight advance of the right leg.

1054 DIV Date: 17th to 19th century AD Production: China (?); India (?)	
Small ivory bottle of approximately cylindrical shape and convex cap.	

1055 DIV Date: 17th to 19th century AD Production: China (?); India (?)	
Small ivory bottle of approximately cylindrical shape and convex cap.	

1043 DIV Date: 18th to 19th century AD Production: China	
Small perfume bottle ivory. It is approximately shaped cylindrical, narrowing at the top. High cap ending in pinecone. Striated and leaves decoration. Stylized.	

167 ESC Date: 18th century AD	

Standing and frontal, the figure has an uncovered head and short wavy hair. Of Head

low, with a slight twist to the right, she wears a smooth tunic, structured in strong parallel vertical pleats with a curved profile hiding her feet. With three-quarter sleeves and a round neck, the tunic is cinched at the belly by a double loop band falling in points. Static. Massive sculpture.

1061 DIV Date: 18th to 19th century AD Production: India (?)	
Piece in bone, with a circular base, turned foot and circular receptacle, perforated and surmounted by a cross removable. one of the parts of the receptacle is removable.	

1042 DIV Date: 18th to 19th century AD Production: China	
Perfume bottle, small in turned ivory. and of approx. cylindrical, narrowing at the top. Tall and narrow lid. Striated decoration and stylized leaves.	

São Roque Antiguidades e Galeria de Arte

SR_ES2 Date: 17th century Production: Sinhalese-Portuguese	

Rare Saint Anthony ivory statuette characterized by the Baby Jesus seated in a Lotus-like seat position clearly inspired by local Buddhist traditions.

The image, of clear Mannerist flavour, stands on a shallow diamond pattern edged socle. The face, oval, is portrayed with low gazing contemplative oblong shaped eyes. The hair is carved in delicately incised grooves framing the tonsure. The Saint's habit is plainly but carefully carved, the capuche falling on the back beneath the raised cowl as per conventional Franciscan rule, and tied at the waist by a cord with pending tips and the three knots symbolizing the Order's vows of poverty, chastity and obedience.

St. Anthony is depicted with his standard attributes; on the left arm he holds the Baby Jesus seated on the Sacred Book, while the right hand would have held the lily stems, alluding to purity, which are no longer present.

The Baby Jesus is shown in his Salvator Mundi appearance, blessing the faithful, with semi closed eyes, tranquil expression and enigmatic smile, seated on a book, his legs flexed, inspired by the iconography of the meditating Buddha (

SR1 Date: 17th to 18th century Production: Western Africa, Sapi-Portuguese(?)	

A rare ivory Oliphant, or hunting horn, most probably made in West Africa's Sierra Leone region. Of sober decoration, the plain faceted body of octagonal section and the marked light coloured ivory border, probably due to the previous existence of a silver mounting, contributing to its rarity and conferring it sophistication and elegance.

In the shorter curvature, a small carved ring for suspension during transport or use. On the outer surface, near the top, two small orifices for blowing. A triple ring, ornamented with incised zigzagging parallel lines, isolates the horn from a simulated mouth piece.

PH_ES1 Date: 17th century Production: Manila, Philippines (?)	
Ivory sculpture of Michael Archangel slaying the devil, with marked Oriental features possibly made under Chinese models in the Philippines for the Spanish market. Facial features display markedly painful expressions, even more so than Portuguese models.	

CH_ES1 Date: 17th century Production: China (?)	
Ivory Virgin possibly of Chinese origin, representing the Immaculate Conception, with the infant Jesus on her arms.	

CH_ES2 Date: 17th century Production: China (?)	
Carved ivory frame possibly of Chinese origin, featuring a scene of the Our Lady of the Rosary, surrounded with angels and devotees.	

IP_ES1 Date: 17th century Production: Indo-Portuguese (?)	
Indo-Portuguese Good Shepherd ivory from Goa, with the clothed Christ at the stop and a reclined figure at the base.	

IP_ES2 Date: 17th century Production: Indo-Portuguese (?)	
Indo-Portuguese Ivory Virgin – representing the Immaculate Conception, with gilding over the edges of the robe.	

IP_ES3 Date: 17th century Production: Indo-Portuguese (?)	

Indo-Portuguese polychrome ivory of the Crucified Christ with red paint and varnished.

SR2 Date: 16th to 17th century Production: Indo-Portuguese (?)	

Indo-Portuguese ivory Oliphant or hunting horn, wit

A rare ivory Oliphant, or hunting horn, most probably made in West Africa's Sierra Leone region. Of sober decoration, the plain faceted body of octagonal section and the marked light coloured ivory border, probably due to the previous existence of a silver mounting, contributing to its rarity and conferring it sophistication and elegance.

In the shorter curvature, a small carved ring for suspension during transport or use. On the outer surface, near the top, two small orifices for blowing. A triple ring, ornamented with incised zigzagging parallel lines, isolates the horn from a simulated mouth piece.

SR_ES2 Date: 15th to 16th century Production: Sri Lanka (?)	

Ivory Virgin from Ceylon, displaying typical Sri Lankan facial features. Hands crossed in prayer as she stands on a crescent moon, and mounted on the same ivory base.

TL_ES1	
Date: 16th to 17th century Production: Thailand (?)	
Ivory Infant Christ in a reclining position reminiscent of the reclining Buddha in Hinduist cultures.	

TL_ES2	
Date: 17th century Production: Thailand (?)	
Ivory Infant Christ in a reclining position reminiscent of the reclining Buddha in Hinduist cultures, with the head resting on a skull. It might signify the cycle of death and life.	

Private Collections

AV_ES2 or AV_OL1	
Date: Late 17th to early 18th century AD Production: Indo-Portuguese	
Indo-Portuguese Ivory Virgin from Goa - Late 17th / early 18th century, representing the Immaculate Conception, standing on a crescent moon, adorned with one angel heads, with baby Jesus on her arms.	

AV_ES1 Date: 20th century Production: Asian (?)	
Carved tusk with details of Japanese rural scenes. From António Candeias' private collection, most probably of Asian origin and from the 20th century.	

AV_FG1 Date: 20th century Production: Asian (?)	
Ivory carved letter opener of Asian typology, with the top of the blade carved with a row of elephants, the handle adorned with a leaf pattern and completed with an elephant in the handle.	

IP_BJ1 or AV_BX Date: Not specified Production: Indo-Portuguese	
Ivory box of possibly Indo-Portuguese origin from Goa, with metal adornments in the center and the edges.	

IP_BJ2 or AV_IJ Date: Not specified Production: Indo-Portuguese	
Indo-Portuguese Ivory Christ in reclining position, adorned with bracelets and anklets, with a finger positioned at the lips.	

IP_BJ4 or AV_KN Date: Not specified Production: Indo-Portuguese	
Indo-Portuguese ivory letter opener from Goa, with blue stamp, and the handle adorned with flowers and leaves.	

IP_BJ4 or AV_KN Date: Not specified Production: Indo-Portuguese	
Indo-Portuguese scrimshaw from Goa, embellished with the HMS Royal George (after the 16th century) and a portrait of King George III (not shown).	

IV_CST or IV_BJ3 Date: Not specified Production: Indo-Portuguese	
Indo-Portuguese Ivory Crucified Christ on a wooden cross (not shown) from Goa.	